EL SEVIER

Contents lists available at ScienceDirect

Materials and Design

journal homepage: www.elsevier.com/locate/matdes



Roles of chemistry modification for laser textured metal alloys to achieve extreme surface wetting behaviors



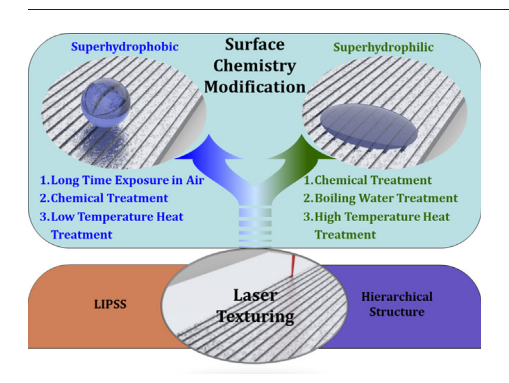
Avik Samanta ^a, Qinghua Wang ^a, Scott K. Shaw ^b, Hongtao Ding ^{a,*}

- ^a Department of Mechanical Engineering, University of Iowa, Iowa City, IA 52242, USA
- ^b Department of Chemistry, University of Iowa, Iowa City, IA 52242, USA

HIGHLIGHTS

- Laser-induced surface structures and following surface chemistry modification are equally critical for extreme wettability.
- Underlaying mechanisms of surface chemistry modification are explained.
- Recent progress in durability laser textured extreme wetting surface is addressed.
- It provides a comprehensive guidance for fabricating extreme wetting surfaces for metal alloys by laser texturing methods.

GRAPHICAL ABSTRACT



ARTICLE INFO

Article history: Received 27 January 2020 Received in revised form 19 March 2020 Accepted 20 April 2020 Available online 30 April 2020

Keywords: Laser surface texturing Chemistry modification Metal alloy Superhydrophobicity Superhydrophilicity Silane treatment

ABSTRACT

Wetting behaviors of structured metal surfaces have received considerable attention due to the wide range of applications for commercial, industrial, and military uses as well as fundamental research interests. Due to its adaptability, precision, and ease of automation, laser-based texturing techniques are desirable platforms to create micro- and nano-structures, including laser-induced periodic surface structures, or hierarchical structures on a metal substrate. However, micro- and nanostructures alone often do not achieve the desired wettability. A subsequent surface chemistry modification method must be performed to attain target extreme wettability for laser textured metal substrates. This review aims to provide a systematic understanding of the interdependence of surface chemistry modification and physical surface structures formed during the laser-based surface engineering methods. The role of surface chemistry on top of the surface structures is presented to decide the final wetting scenario. Specifically, by controlling the surface chemistry of a laser textured surface, wetting can be modulated from extreme hydrophobicity to hydrophilicity, allowing freedom to achieve complex multi-wettability situations. In each section, we highlight the most fruitful approaches and underlying mechanisms to achieve a fitting combination of surface structures and surface chemistry. Durability and stability of the treated surface are also discussed in corrosive and abrasive environments. Finally, challenges in current studies and prospects in future research directions of this rapidly developing field are also discussed. This review will provide a comprehensive guideline for the design of laser texturing methods and the fabrication of extreme wetting surfaces for metal alloys.

© 2020 The Authors. Published by Elsevier Ltd. This is an open access article under the CC BY-NC-ND license (http://creativecommons.org/licenses/by-nc-nd/4.0/).

* Corresponding author.

E-mail address: hongtao-ding@uiowa.edu (H. Ding).

Contents

1.	Introd	duction
2.	Laser	texturing for surface micro-/nanostructures
	2.1.	Laser-induced periodic surface structures (LIPSS)
	2.2.	Hierarchical surface structures
	2.3.	Random nanostructures
3.	Surfac	ce chemistry modification
	3.1.	Long time exposure in air
	3.2.	Chemical treatment
	3.3.	Heat treatment 14
	3.4.	Boiling water treatment
	3.5.	Discussion on durability of laser textured surface with chemistry modification
		3.5.1. Corrosion resistance
		3.5.2. Abrasion resistance
4.		lusions and future perspective
CRe	diT autl	chorship contribution statement
Ackı	nowled	lgments
Refe	rences	

1. Introduction

Employing engineering methods to achieve extreme wettability conditions on metal alloys through creating micro-/nano-scale features along with appropriate chemistry has received considerable attention over the past few decades. Those engineered extreme wetting surfaces were often inspired by natural or biological surfaces with specific physical and chemical characteristics. There exist several natural superhydrophobic surfaces with a water-repelling property, including

lotus leaves [1], rose petal [2], water ferns [3,4], water striders [5], butterfly wings [6,7]. On the other hand, superhydrophilic plant surfaces in *Sphagnum* moss [3,4] also exist in nature to capture water from fog, dew, or rain in high altitudes. All of those extreme wetting natural surfaces possess specific shape of micro/nanoscale surface structures along with fitting chemistry that leads to desired wetting conditions to survive in nature [3]. The interaction between engineered micro/nanoscale structures and liquid, especially water, leads to several wetting scenarios, including extremely high, high, low, and extremely low wettability.



Fig. 1. Applications of micro/nanostructured metal surface with extreme wettability. Superhydrophilic surface for dental implant [16] electrolyte wetting of lithium-ion batteries [10], an electrocatalyst for hydrogen evolution [9], water splitting [8], heat pipe wicks [14] and lubrication [12]. Superhydrophobic surface for anti-icing [28], anti-biofouling and antibacterial [18], self-cleaning [26], oil-water separator [20], anticorrosion [24] and drag reduction [22]. Reproduced with permission of the Elsevier [14,16,18], Royal Society of Chemistry (RSC) [8,12,20,26], Nature [9], Springer [10], Cambridge Core [22], Royal Society [24], American Chemical Society (ACS) [28].

Those wettability conditions play a crucial role in many industrial processes and applications, as illustrated in Fig. 1, such as superhydrophilic surfaces for catalysts [8,9], fuel cells & batteries [10,11], tribology & lubrication [12,13], heat pipe wicks [14], dental treatment [15,16], etc., and superhydrophobic surface for antibacterial & anti-biofouling [17,18], oil recovery [19,20], drag reduction [21,22], anti-corrosion [23,24], self-cleaning [25,26], anti-icing & anti-fogging [27,28], and a combination of both for pool boiling [29,30], and microfluidics [31].

Wetting is the ability of a liquid medium to maintain contact with a solid medium due to intermolecular interaction when they are brought together. Wettability of a solid surface is the measure of the degree of wetting at which surface can get wet by a liquid. Static contact angle (θ) is one of a quantitative way to measure wettability at a solid-liquid interface [32]. It is defined as the angle formed at the three-phase line of liquid resting on a solid surface in equilibrium, and it is measured between solid and gas through the liquid. When the liquid is water, the θ is termed as static water contact angle ($\theta_{\rm w}$). In this review, we only focus on wetting by water. As θ increases from 0° to 180°, surface wetting changes from complete wetting to complete non-wetting. The surface wetting by water can be categorized into two main regions; hydrophobicity when θ_w is more than 90°, and hydrophilicity when θ_w is less than 90° [3,33]. Among each region, there are specific ranges for static contact angle to differentiate between general and extreme wetting conditions. In summary, the wetting by water can be categorized into six categories, as shown in Fig. 2: (i) hydrophilic, (ii) superhydrophilic, (iii) superwetting/superwicking, (iv) hydrophobic, (v) superhydrophobic lotus leaf effect, and (vi) superhydrophobic rose petal effect. Surfaces with θ_{w} < 90° show good wetting behavior. If the θ_w falls between 10° and 90°, the surface is designated as hydrophilic (Fig. 2(a)). If θ_w is less than 10°, the surface is considered as superhydrophilic, and the water tends to spread over the surface

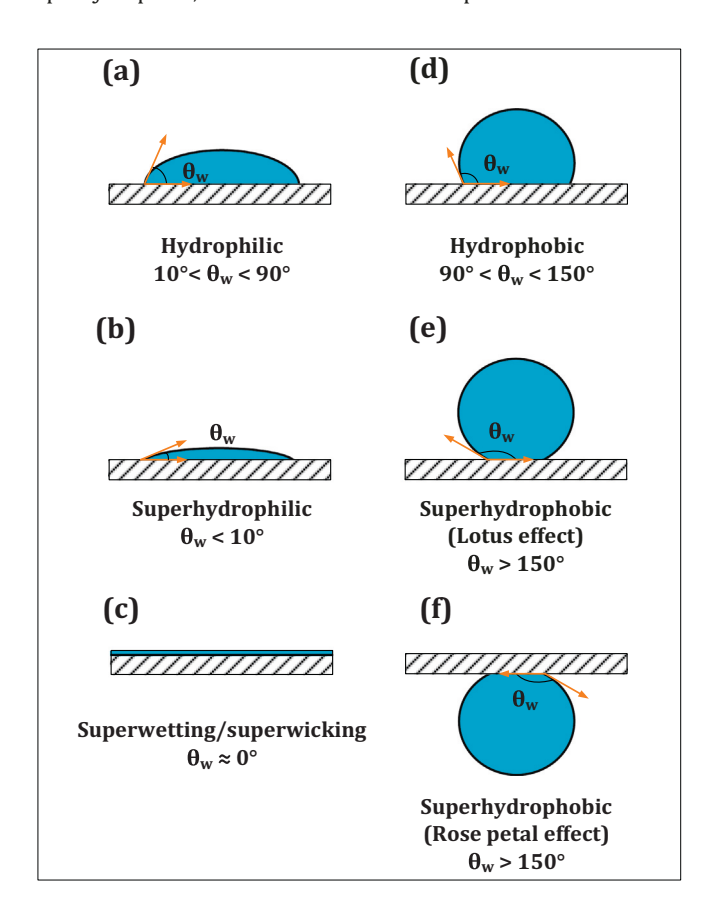


Fig. 2. Classification of wetting based on θ_w : (a) hydrophilic; (b) superhydrophilic; (c) superwetting/superwicking; (d) hydrophobic; (e) superhydrophobic (lotus leaf effect); (f) superhydrophobic with high adhesion (rose petal effect).

(Fig. 2(b)). There is a special category of hydrophilic surface: superwicking surface [34–38], where the θ_w is equal to 0°, as shown in Fig. 2(c). It is also known as a superwetting surface. This is a special case of the superhydrophilic surface where the liquid spreads on the surface at a very high speed as the liquid droplet meets the surface. Liquids also tend to climb against gravity on this kind of surface when kept in a vertical orientation. Surfaces with $\theta_w > 90^\circ$ indicate non-wetting behavior, and static contact angle alone is inadequate because it cannot evaluate the sliding properties of the liquid on the surface. Two additional parameters are used to define the non-wetting behavior of the surface, including roll-off angle ($\theta_{Roll-off}$) and contact angle hysteresis (θ_H) . $\theta_{Roll-off}$ is a critical inclination angle at which the liquid droplet trends to slide/roll off the surface [39]. θ_H is defined as the difference between the advancing contact angle and receding contact angle [40]. Surfaces with $150^{\circ} < \theta_{w} < 90^{\circ}$ are categorized as hydrophobic (Fig. 2(d)). When the hydrophobicity increases, θ_w of the droplets with the surface increases as well. When θ_w is higher than 150°, the surface is generally recognized as superhydrophobic. There are two kinds of superhydrophobic surfaces including superhydrophobic "lotus leaf" and "rose petal" as shown in Fig. 2(e) and (f) respectively. For superhydrophobic "lotus leaf" surface, water droplets tend to slide off the superhydrophobic lotus leaf effect surface if the surface is tilted at a small angle. It requires to have low $\theta_{Roll\text{-}off}$ (<10°) [39] and low θ_{H} (<10°) [41,42]. On the other hand, a superhydrophobic "rose petal" surface usually possesses high adhesion force [43,44], where water droplet sticks on the superhydrophobic surface, although the surface is tilted upside down ($\theta_{Roll-off} > 90^{\circ}$) as shown in Fig. 2(f). It usually have $\theta_{Roll-off} = \theta_{Roll-off} = \theta_$ $_{\rm off} > 90^{\circ} [45]$ and $\theta_{\rm H} > 10^{\circ} [46]$.

The wetting process of solids was first analytically expressed using a simple model using Young's equation to describe the equilibrium condition of a liquid droplet on an ideal solid surface, as shown in Fig. 3a.

$$\cos(\theta) = \frac{\gamma_{sv} - \gamma_{sl}}{\gamma_{lv}} \tag{1}$$

where γ is the surface tension that indicates the energy per unit surface area of the interface, the subscripts sv, lv and sl signify solid-gas, liquidgas, and solid-liquid interfaces, respectively. Validity of this equation is limited to a smooth, chemically homogeneous, rigid, insoluble, non-reactive infinitely flat surface. Although all the real surfaces are not ideal, Young's equation provides a basic understanding of the relationship between static contact angle and interfacial surface tensions. For the rough real-world surface, two main wetting regimes are considered throughout the literature, i.e., Wenzel [47] and Cassie-Baxter [48] wetting regime. In the Wenzel regime, liquid droplet moves inside the surface roughness, and the real surface area increases due to roughness, as shown in Fig. 3b. Consequently, the actual interfacial area between the solid and liquid medium is much higher than the apparent geometric contact area, which makes the surface hydrophobicity level to increase compared to a smooth surface. The apparent contact angle (θ^*) was proposed as:

$$\cos(\theta^*) = r_f \frac{\gamma_{sv} - \gamma_{sl}}{\gamma_{lv}} = r_f \cos(\theta)$$
 (2)

where, $r_f(r_f>1)$ is the solid surface roughness factor, which signifies the ratio of solid surface area to the projected area. In Cassie and Baxter regime, liquid droplet does not penetrate the surface roughness, and some gas is entrapped in between the liquid and solid, as shown in Fig. 3c. That makes the solid-liquid interface as a combination of the solid-liquid and solid-gas interface. Only a fraction f(0 < f < 1) of r_f contributed towards the solid-liquid interface, the apparent contact angle can be given by [49],

$$\cos(\theta^{**}) = r_f f \cos(\theta) + f - 1 \tag{3}$$

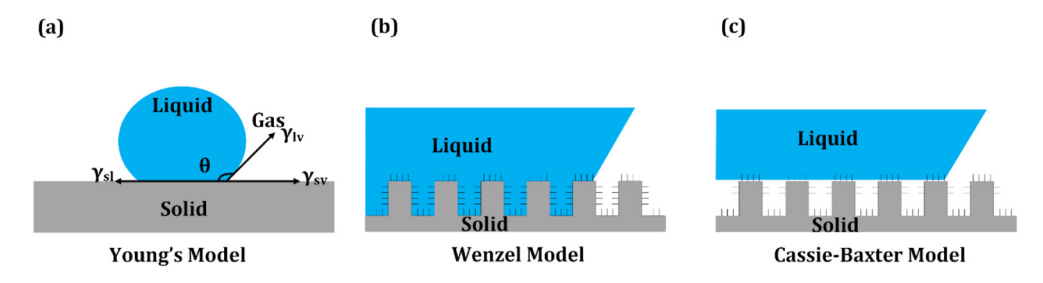


Fig. 3. Wetting Models. (a) Young's model; (b) Wenzel model; (c) Cassie-Baxter model.

However, both of these regimes only contemplate the interfacial surface tension as one factor and do not consider the various components of surface chemistry that influence interfacial surface tension.

Wetting scenarios based on the roughness modification can be summarized in Table 1. For a surface with hierarchical roughness with smaller nanostructure on top of larger microstructure, several wetting scenarios can be reached, including Wenzel, Cassie-Baxter, and intermediate metastable regimes [46]. Water can penetrate either into the micro- or nanostructure or into both. When the surface has a high dual roughness with deep microstructures combined with rich nanostructures, a layer of air is trapped between the surface and the droplet. Thus, it leads eventually to high θ_w , low $\theta_{Roll-off}$ and low θ_H , which leads to a superhydrophobic lotus leaf effect. When the surface microstructures become shallower, some parts of water droplet can partly get into the microstructure, and the wetting state becomes an intermediate metastable or combined state [46,50]. The increased liquid-solid contact area results in an enlarged adhesion to water. On this surface, water could infuse into part of microstructures, but it still does not entirely wet into the nanostructures, resulting in high $\theta_{Roll-off}$ and θ_{H} while maintaining high θ_w [46]. When the surface microstructures become shallower, the water droplet can get into the grooves of the rough solid surface completely, leading to the Wenzel regime. Thus, the θ_{w} decreases, and $\theta_{\text{Roll-off}}$ and θ_{H} increase rapidly.

There are two main forces, i.e., adhesive force and cohesive force, that contributed towards the interfacial interactions. The adhesive force between a liquid and solid medium assists the liquid spreading, and cohesive forces within the liquid molecules resist contact with the solid surface [32]. The adhesive force at the liquid-solid interface and cohesive force of the liquid compete against each other to decide the wetting scenario at the interface. If the adhesive force at the solid-liquid interface is stronger than the cohesive force of the liquid, good wetting happens. On the other hand, if the cohesive force is stronger than the adhesion force at the interface, liquids tend to form a droplet, and the surface behaves as non-wetting or partial wetting. In general, a specific liquid effectively wets solid surfaces with high γ_{sv} value compared with surfaces with low γ_{sv} . The value of γ_{sv} depends on bonding between atoms at the surface layers. For example, metals, ceramics, glasses which are held together by strong cohesive forces due to the presence of ionic, metallic and covalent bonds, possess high γ_{sv} as it requires high energy to disrupt the bonds. On the other hand, hydrocarbons, fluorocarbons which were held together by weak van der Waals and hydrogen bonding forces, have low γ_{sv} as it requires less energy to break those bonds [51]. Again, if the γ_{sv} of solid surface is much higher than

Table 1Different regimes of wetting of a surface with dual roughness.

	Air in microstructure	Water under droplet in microstructure
Air in nanostructure	Ideal lotus effect High θ_w , Low θ_H , Low	Ideal rose effect High θ_{w} , High θ_{H} , High
Water under droplet in nanostructure	$\theta_{Roll-off}$ Cassie state High θ_{w} , Low θ_{H} , Low	$\theta_{Roll-off}$ Wenzel state High θ_{w} , High θ_{H} , High
	$\theta_{ m Roll-off}$	$\theta_{Roll-off}$

 γ_{lv} of liquid, the wetting becomes easier. It indicates the chemical condition of the solid surface contributes significantly on the wetting behavior at the solid-liquid interface.

Therefore, both solid and liquid surface properties are critical at the interface to decide the final wetting behavior [52]. It has been widely researched that the wettability condition of a solid surface can be altered through surface micro/nanostructuring [48,53-56]. In the real world, solid surfaces are not smooth. Surface roughness or surface topography is naturally present or deliberately imposed on the realworld surface during the fabrication process. The surface roughness of a real surface can vary from several micrometers to several nanometers. Surface chemistry of a solid also plays a decisive role in wetting behavior [57]. Specific surface chemistry is also generated or purposefully introduced during the fabrication process, which contributed towards its $\gamma_{\rm sv}$ of the real-world rough surface. External excitation like UV illumination also influence wettability transition for some unique photosensitive oxide semiconductors like ZnO [58,59] and TiO₂ [59] by influencing the surface chemistry. With UV illumination, surface oxygen vacancies are generated in both ZnO and TiO2, which leads to dissociative adsorption of the water molecules in the surface. Based on a specific combination of surface topography and surface chemistry, desired wettability scenario for a solid surface for a specific liquid can be achieved. On the liquid side, liquid-vapor surface tension $(\gamma_{l\nu})$ contribute towards the wettability scenario [60,61]. γ_{lv} is also a function of temperature, therefore temperature of the environment also contributes to the wettability.

It is important to understand how to fabricate the desired topography and impose favorable chemistry on engineering metal substrates for desired wettability. Many engineering methods have been studied to fabricate extreme wetting surfaces based on the two primary factors, including surface chemistry and surface micro-/nanostructures [62,63]. Two main fabrication strategies have been practiced over the years [64,65]. For the first type, surface topography is generated on the substrate material using one process. Subsequently, surface chemistry is created by films and coatings on it through a second process. For the second type, surface topography and surface chemistry are created on the substrate material in one single process though rough film coating [66,67]. All the reagents are mixed to produce the final product with a single process step. A mixture of cobalt salt with n-dodencanethiol formulates metal dodecanethiolates that simultaneously provide surface roughness and surface chemistry for excellent superhydrophobicity [67].

For the first strategy, several techniques inspired by nature have been used to produce micro/nanoscale surface topography. These techniques to create surface structures are categorized into three main approaches: (a) top-down approach which removes material selectively or randomly from the base material to create nano or micro-scale surface structures. High-intensity thermal energy sources and chemical or electrochemical reactions [68–72] are used to remove materials. Processes with top-down approach include chemical etching [70,73,74], plasma etching [75], laser texturing [76–78], lithography [79]. (b) A bottom-up approach which creates nanoscale features on top of the base material by building up atom by atom or molecular scale components [80,81]. This approach includes electrochemical deposition

[82–86], electrospinning [87], anodic oxidation [88], and layer-by-layer (LBL) deposition [89,90], sol-gel method [91]. (c) A combination of topdown and bottom-up approaches [92] which takes the advantages of both top-down and bottom-up approaches to generate surface structures. Several combinations have been explored, including etching with KOH, and Au nanoparticle catalyzed HF/H₂O₂, followed by the sol-gel method [93] on silicon. A combination of photolithography for micropillar arrays and chemical vapor deposition (CVD) of anisotropically aligned carbon nanotubes was used to create hierarchical structures on a silicon substrate [94]. Nanostructure alone cannot produce desired wettability, so a chemistry modification technique is required after the nanostructure generation or simultaneously during the nanostructure generation. After the surface structure generation, surface chemistry modification techniques are applied, which include the solgel method [91,95], chemical vapor deposition [96,97], chemical immersion [98], etc.

In the last decade, laser-based surface processing methods emerged as one of the widely researched areas of the top-down approach to create micro/nanoscale surface structures. Remarkable progress has been made in laser material processing research on both fundamental knowledge and fabrication points of view [45,68,99-102]. Processing with pulsed laser is a contactless material removal method that irradiates the substrate surface by single or multiple laser pulses. These techniques have several unique features that make it an exciting choice for surface topography generation for metals due to ease of automation, reliability, repeatability, and controllability. Extensive knowledge has been obtained on the design and manufacturing of extreme wetting surfaces, i.e., superhydrophobic [21,103-109] and superhydrophilic surfaces [110-115], however, most of the existing literature reviews only discussed the fabrication strategies of laser-based processes [21,102,104,107,114–116]. These articles only stressed on the types of surface structures created by laser irradiation.

Immediately after laser texturing of engineering alloys, textured surface usually behaves as superhydrophilic [100,117,118]. Laser processing of metal generates metal oxide on the textured surface as it is a high energy processing. Metal oxides are typically hydrophilic because their electronic structure favors the formation of hydrogen bonds [119]. Metal oxides possess higher surface energy. For instance, immediately after laser treatment, the AA6061 surface contains Al₂O₃ and the aluminum atoms at the surface are electron deficient, resulting in a formation of a hydrogen bond with interfacial water molecules Therefore, the surfaces behave as superhydrophilic immediately after laser texturing. This superhydrophilicity is stable if the textured surface is stored in N2, CO2, or O2 environment [100]. Surface energy remains high in those environments. However, it is unstable if it is exposed to air [100] or vinegar, sodium bicarbonate solution, IPA, and saltwater [120]. It undergoes a transition from superhydrophilicity to superhydrophobicity within a period of 8-30 days [100,117,118]. Exposure to different medium accelerates or decelerates the wettability transition process [120]. IPA accelerated wettability transition, whereas sodium bicarbonate slowed it down. Due to this exposure, the surface adsorbs organic molecules, which modifies the surface chemistry permanently, leading to superhydrophobicity [100]. Earlier work reported on laser textured superhydrophobic surfaces did not consider the effect of storage in air as a chemical modification. It claimed to be achieving superhydrophobicity without chemical modification after laser texturing. However, recent work explains the mechanism of attachment of long hydrocarbon chain of organic molecules exposure to atmosphere leading to wettability transition [100,118]. Author's group recently have shown that several extreme wetting scenarios can be achieved on samilar laser textured surface by controlling the dispersive and non-dispersive components of surface chemistry [230]. Those extreme wettabilities include superhydrophobicity, superoleophobicity, superhydrophilicity, superoleophilicity and coexistence of superoleophobicity and superhydrophilicity.

Although the wetting behavior of a laser textured metal surface is a complex combination of surface chemistry and surface topography, most of the existing literature only explored the generation of physical topographical changes, i.e., micro-/nano-scale surface structures by lasers. A significant knowledge gap exists in the current literature on the importance of surface chemistry alongside laser-textured surface structures.

This review intends to examine the roles of surface chemistry modification for laser texturing processes of metal alloys to achieve desired extreme wettability, and hence solely focuses on the material processing science. The goal of the review is to provide a systematic understanding of the interdependence of surface chemistry modification and surface structure generation during the laserbased surface engineering methods of metals and metal alloys. While applications of extreme wetting surface and their durability under various environmental loadings are of great interest, these topics are out of the scope of this review. In Section 2, we will review the existing laser textured surface structures of metals and metal alloys to provide a background for the following surface chemistry modification processes. In Section 3, we will review the underlying mechanisms of the existing surface chemistry modification techniques used to decide the final wettability scenario. Finally, in the last section, we will provide concluding remarks and future research directions. The review is, as a matter of fact, a very first review work to systematically discuss the role of surface chemistry and the methods for surface chemistry modification for laser surface texturing of metals. The review also helps provide a guideline for the design of laser texturing methods and fabrication of extreme wetting surfaces for metals and alloys.

2. Laser texturing for surface micro-/nanostructures

Laser direct writing to create textures on the substrate is the most frequently used approach for the fabrication of extreme wetting surfaces due to the ease of processing setup and operation [121]. The fabricated surface structures depend on laser processing parameters (pulse energy, repetition rate, pulse duration, scanning speed, wavelength, processing environment, polarization, etc.) and substrate material properties (thermal conductivity, specific heat, bandgap, etc.) [122,123]. The pulse width of those lasers can range from a few nanoseconds to a few femtoseconds with a wavelength ranging from 355 nm (UV laser) [98] to 1064 nm (IR laser) [100]. Repetition rate ranging from 10 Hz [124] to 10^6 Hz [125] has been used to texture engineering metals and metal alloys. During laser processing, different environment is also explored, including air, CO_2 , O_2 , O_2 , O_3 , O_4 , ar, water [124,126].

The classification of laser textured surface structures and their generation approach can be seen in Fig. 4. Almost all of the developed laser texturing methods follow the top-down approach, which inherently creates nanoscale laser-induced periodic surface structure (LIPSS) or hierarchical/dual scale structures, i.e., both microscale and nanoscale structures [68,127,128,208], in an exact local region of the target surface and then processes the whole surface area by scanning the laser. A wide range of pulsed laser with pulse duration in nanosecond (10^{-9}) [72,129], picosecond (10^{-12}) [77,100], and femtosecond (10^{-15}) [76,130] has been used to produce surface structures on metals. Hybrid laser texturing techniques [131,132] are also used to create hierarchical surface structures where microscale structures are created by nanosecond pulsed laser, and nanoscale features are created by femtosecond or picosecond pulsed laser. In addition to these developed topdown laser texturing methods, a newer combined approach has recently been developed to create randomly distributed nanoscale structures. It uses a rapid nanosecond laser scanning process to precondition the target surface without generating the usual micro/ nanostructures and then applies chemical treatment to process the whole surface [124,133].

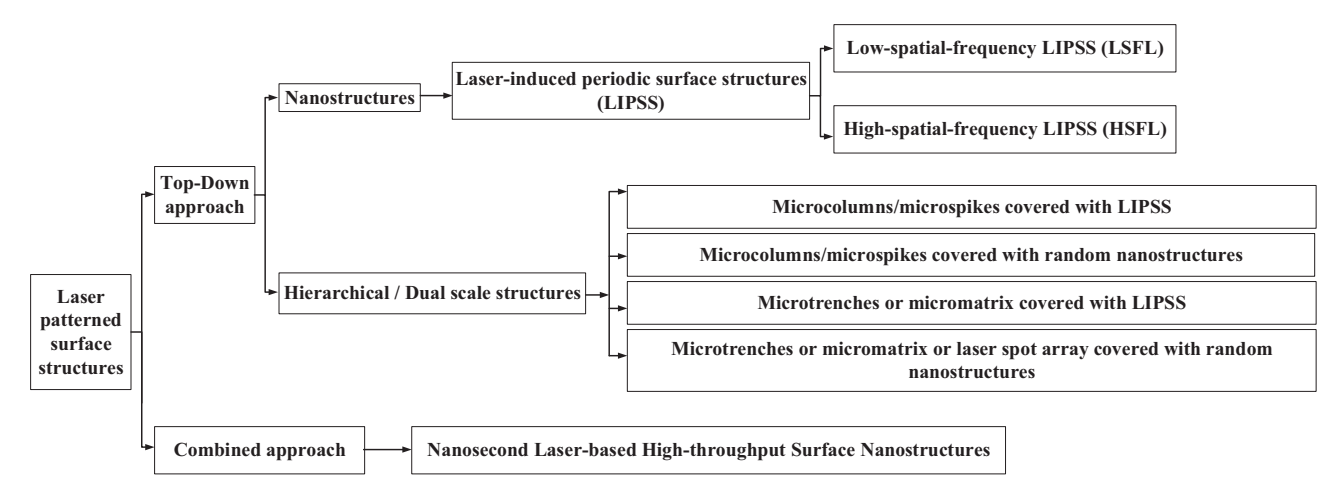


Fig. 4. Classification of fabrication approach and surface structures created by laser texturing.

2.1. Laser-induced periodic surface structures (LIPSS)

Femtosecond and picosecond laser-based texturing methods can create nanometer-scale surface structures using a top-down approach by removing material selectively by an ultrashort pulse laser source. These nanostructures generally are known as LIPSS. LIPSS appears on solids during irradiation with linearly polarized laser radiation [134,135]. Birnbaum [136] first observed this in 1965 on several semiconductor surfaces irradiated by ruby-laser. These surface structures can be fabricated on a wide range of materials, including semiconductors, metals, and dielectrics [137]. LIPSS is formed in a wide range of pulse duration ranging from several picoseconds [138] to several femtoseconds [139]. When the laser fluence is very close to or little above the ablation threshold value of the target material, a periodic nanoscale LIPSS structures will appear. LIPSS generally composed of periodic lines of nanoscale surface structures that display a clear correlation with the polarization of laser radiation and wavelength. The periodicity of the LIPSS is equal to or smaller than the wavelength of the laser radiation, and it is much smaller than the effective laser spot size [127]. There are two main categories of LIPSS structures generated during pulsed laser irradiation, i.e., Low Spatial Frequency LIPSS (LSFL) and High Spatial Frequency LIPSS (HSFL). LSFL is formulated as a result of the periodic spatial distribution of the laser pulse energy. According to the classical theories [137,140], LSFL is generated due to the interference between the incident laser beam and rough surface-induced surface electromagnetic waves, including the excitation of the surface plasmon polaritons [141–143]. Its periodicity (Λ_{LSFI}) is usually close to the laser wavelength (λ) or λ/n ($\Lambda_{LSFL} \approx \lambda$ or λ/n), where n is the refraction index of the material. Table 2 lists down a summary of fabricated LSFL on different metal and metal alloys with their periodicity and threshold fluence used to generate the features. On the other hand,

Table 2 LIPSS reported on different metals and metal alloys with their fluence and periodicity (λ/n) .

Material	Fluence (J/cm ²)	Periodicity ratio (λ/n)	Reference
AISI 316L steel	0.08-0.2	1.60	[145]
	2.04	1.45	[147]
SS304	0.4-1.1	1.33	[148]
Al	0.05	1.48	[149]
Cu	0.15-2	2.00-1.18	[150]
Ti	0.25	1.14	[151]
	0.09-0.45	1.6-1.14	[152]
	0.067-0.084	1.51	[127]
Ti Alloy	2.04	1.33	[147]
Ni	0.12	1.33	[153]
	0.97-1.42	1.82-1.43	[141]

HSFL has a periodicity smaller than half of the laser wavelength $(\Lambda_{\rm LSFL} < \lambda/2)$ and can be either perpendicular or parallel to the polarization of the incident laser beam. Fundamentally, the formation of LIPSS is a complex process that comprises a sequence of physical movement of materials during inter- and intra-pulse duration. The laser radiation is absorbed by the electronic system of the target material and the delivered energy transferred into the lattice system of the solid, leading to thermal, hydrodynamic, and chemical events [135]. Those events eventually affect the formation of periodic structures through spatially modulated material ablation and re-solidification. There are conflicting theories on some aspects of that physical phenomenon. Due to the complexity and interdependency of all the physical events in a short span of time of laser irradiation, a comprehensive theory of LIPSS formation is not present at this point of time.

From the processing point of view, the fabrication of LIPSS is straightforward compared with the complexity of the formation mechanism. In one step, nanostructures are generated that facilitates the functionalization of the surface towards optical, mechanical, biological surface properties. The formation of LIPSS is affected by both laser texturing parameters and target material physical properties [144]. Li et al. [76] and Bo et al. [145] studied the effect of laser fluence on LIPSS formation using femtosecond laser on pure titanium and stainless steel, respectively. At lower laser fluence, only LIPSS is observed; however, at higher fluence, the surface structures transform from LIPSS to hierarchical/dual scale shape. Fig. 5a illustrates the transformation of LIPSS structures to conical-shaped spikes covered with LIPSS as laser fluence increased. With the increase of laser fluence, the height and distance between spikes are also increased [76,145]. No. of pulses also plays a crucial role in the LIPSS formation for femtosecond laser [127,146]. At a lower number of laser pulses, only LIPSS is observed, whereas, at a higher number of laser pulses, bimodal roughness can be fabricated, where microcolumns are covered with LIPSS (Fig. 5b). For all the fabricated LIPSS structures, surface chemistry modification is required to achieve extreme wettability.

Nanostructure plays a very important role in establishing the final wettability. Laser fluence, no. of pulses, and the processing environment play a very important role in deciding the nanostructure size and distribution. With very low laser fluence and no. of pulses, the nanostructures are random. With increasing laser fluence and no. of pulses, the randomness disappears, and periodic LIPSS emerges. Beyond a certain threshold value of laser fluence and no. of pulses depending on the target material, LIPSS disappears, and dual scale microspikes or microcolumns covered with LIPSS shows up. Without chemistry modification treatment, $\theta_{\rm w}$ on the LIPSS structure decreases as the laser fluence increased and eventually becomes superhydrophilic with $\theta_{\rm w}=0^\circ$ [76] after a threshold laser fluence. After chemistry modification, $\theta_{\rm w}$ on LIPSS increases with laser fluence [76] to more than 150°.

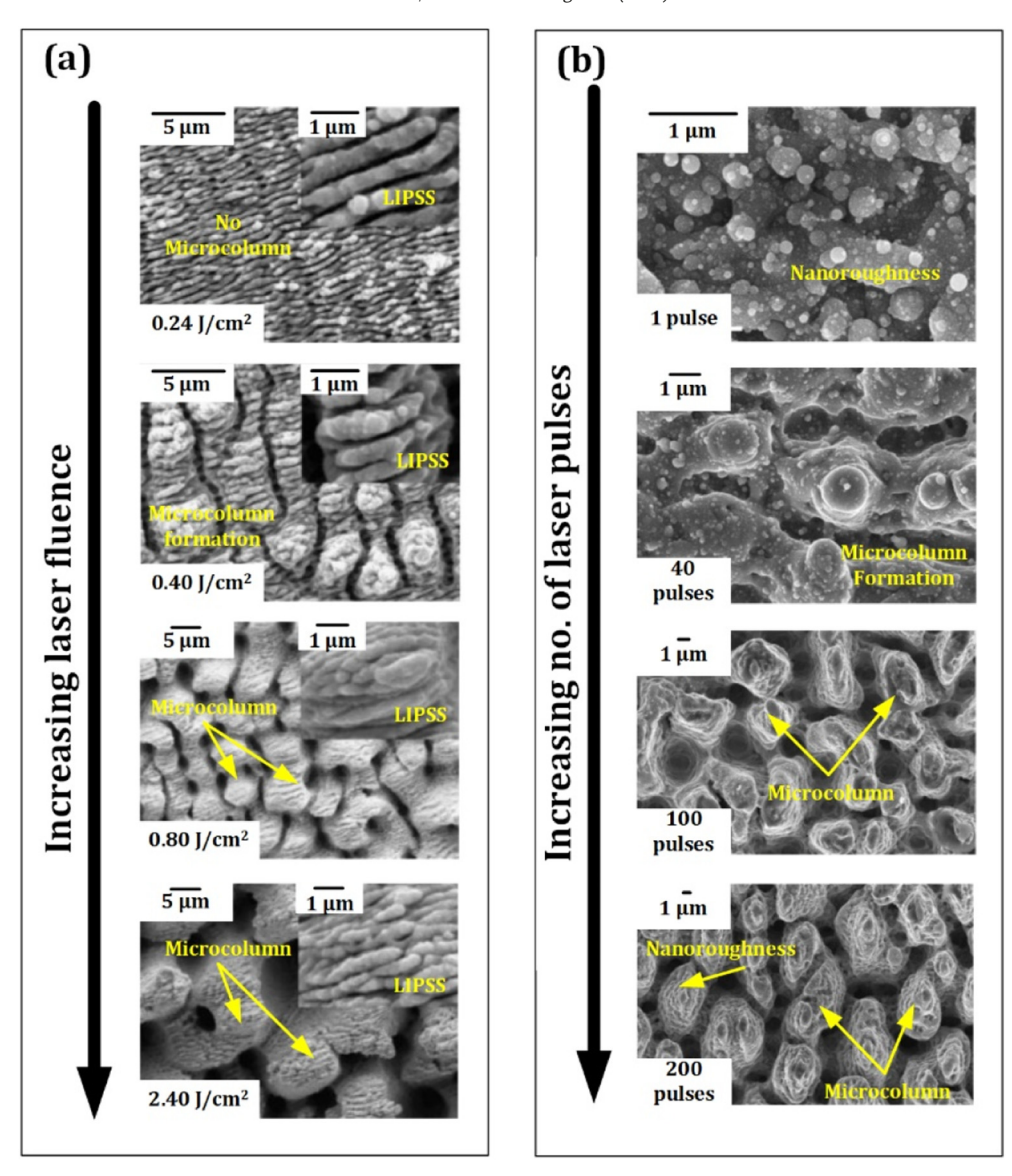


Fig. 5. LIPSS formation at different processing parameters and transformation to hierarchical structures; (a) change of LIPSS to hierarchical structures with increasing laser fluence. Reproduced from [145] with permission of the Elsevier. (b) change of LIPSS to hierarchical structures with increasing no. of pulses at the target location. Reproduced from [127] with permission of the Elsevier.

2.2. Hierarchical surface structures

Hierarchical structures or dual-scale micro/nano surface structures are also fabricated on the target substrate through various laser texturing strategies. The hierarchical surface structure typically consists of one structure at a higher scale (micron scale) and another structure at a lower scale (nanoscale) on top of higher scale structures. Those structures can be categorized into four main classes based on their fabrication strategies, as shown in Fig. 6. They are (a) microcolumns or spikes covered with LIPSS, (b) microcolumns or spikes covered with random nanostructures, (c) microtrenches, or micromatrix covered with LIPSS and (d) microtrenches or micromatrix or laser spot array covered with random nanostructures. When the laser fluence is very high, much above the ablation threshold value of the target material, a disruptive modification occurs, resulting in microcolumns or spikes covered with LIPSS structures [76,142,145,154]. Wu et al. [145] show that stainless steel surface textured with cone-shaped spikes covered with LIPSS structures had enhanced wetting performance compared to only nanoscale LIPSS. Long et al. fabricated coneshaped microprotrusions or microcolumns covered with random nanostructures using femtosecond laser at a very low scanning speed [45,155]. They scan the surface in the horizontal direction, followed by in transverse direction to create a hierarchical structure at the intersection region. They needed to do chemistry modification after the surface structure generation to achieve both superhydrophobic lotus and rose petal effect. The third kind of hierarchical surface structure is created by laser irradiating the surface in two separate passes. In the first pass, microtrenches/microgrooves or micromatrix/crosshatch were created on the metal substrate, and in the second pass, LIPSS were generated on the micronscale structures [131,132,156]. The textured surface also required chemistry modification after the texturing process to achieve superhydrophobicity. The fourth kind of hierarchical structures created by single-step laser irradiation [68,69,72,129,157,158]. Microscale surface microtrenches/microgrooves [68,72] or micromatrix/crosshatch [69,158] or spots array [129,157] were created by pulsed laser irradiation. The random nanoscale features on top of the microscale features were created by solidified ablated materials.

Hierarchical/Dual-scale Surface Structures 1. Microcolumns / Spikes 2. Microcolumns / Spikes 3. Micro-trench / Micro-matrix 4. Micro-trench / Micro-matrix / (Higher Scale) (Higher Scale) (Higher Scale) Spot array (Higher Scale) LIPSS (Lower Scale) Random Nanostructure LIPSS (Lower Scale) Random Nanostructure (Lower (Lower Scale) Scale) Higher Higher 10 um Lower

Fig. 6. Different types of laser textured hierarchical surface structures; (1) Microcolumns/spikes covered with LIPSS, Adapted from [154] with permission of the Elsevier. (2) Microcolumns/spikes covered with random nanostructure, Adapted from [45] with permission of the ACS. (3) Micro-trench/micro-matrix covered with LIPSS, Adapted from [132] with permission of the Elsevier. (4) Micro-trench/micro-matrix/spot array covered with random nanostructure. Adapted from [157] with permission of the Elsevier.

2.3 Random nanostructures

Random nanostructured surface produced by top-down approach normally consists of nanocavities, nanoholes, nanobumps, and nanoprotrusions. Due to the very short interaction of metals with ultrafast lasers, localized nanoscale melt, bubble cavitation, and nanoparticle redeposition happen, which leads to random nanostructure generation [127,159]. Random nanostructures were generated at a low laser fluence which is near the ablation threshold of the target material and at a very low number of pulses at the irradiation spot [127,130]. The size of nanoscale surface features increases with increasing fluence with fixed laser pulses and increasing number of pulses with fixed laser fluence [127,130]. However, after chemistry modification, the contact angle stays below 150° on this kind of random structures prepared by the top-down approach [145].

Recently, a combined approach has been developed to generate random nanostructure using the Nanosecond Laser-based Highthroughput Surface Nanostructuring (nHSN) process [124,133]. nHSN consists of two sequential steps. The first stage performs water confined nanosecond laser texturing (wNLT) to prepare the metal surface both chemically and mechanically. This stage does not generate the final topological patterns. The second stage is chemical immersion treatment (CIT). In this stage, the chlorine atoms in the chlorosilane reagent react with the laser textured metal surface to induce simultaneous chemical etching and attachment of functional groups [124]. As a result, the generation of surface nanostructure and surface chemistry occur simultaneously within the CIT stage. These results show that surface nanostructuring with proper chemical attributes results from a combined effect of chemical etching and attachment of functional groups during the CIT phase of nHSN. The metal surface treated with the nHSN process exhibits a unique surface structure consisting of random nanostructures of various protrusions and cavities ranging from several tens to several hundreds of nm, as shown in Fig. 7. The final nanostructure was not generated after the completion of the wNLT process. It was generated after the completion of the CIT process. These surface structures are fundamentally different from those discussed in Sections 3.1 and 3.2. In this technique, random nanostructures and desirable surface chemistry were generated simultaneously over large-area metal alloy surfaces [124,133,160,161]. Water confined nanosecond laser texturing generates randomly distributed microscale surface ripples and pores. Following chemical immersion treatment with chlorosilane on the laser textured AISI 4130 steel produce random structures of various shapes of protrusions, rods, cones, platelets, and pores (Fig. 7) with fluorination chemistry. This simultaneous generation of nanostructure and fitting chemistry is a combined effect of chemical etching and attachment of functional groups during the chemical immersion treatment of laser textured metals/metal alloys [124,133]. Increasing the laser power intensity during the nHSN process results in a feature size decrease and an increase in nanoscale feature density.

It can be concluded that both microscale and nanoscale surface structures play an important role in the final wettability. Only microscale or only nanoscale features usually increase the contact angle hysteresis even for a Cassie state wetting scenario [162,163]. This contact angle lag is assigned to an increase in surface energy, resulting from the changes in microtopography. On the other hand, hierarchical structures with both micro and nano features usually lead to better superhydrophobic wettability with lotus effect [164]. However, all those surface structures on metal and metal alloys single-handedly could not achieve the target wettability. A chemistry modification step was always required to achieve the target wettability.

3. Surface chemistry modification

Favorable chemistry of the nanostructured surface is critical to achieving desired (super) hydrophobic or hydrophilic wetting conditions [165–168]. There are several surface chemistry modification techniques to achieve superhydrophobicity, including anchoring fluorinated groups such as perfluoro-alkanes on the nanostructured surface [98,169], exposing to atmospheric condition for extended periods [100,118,170], and low-temperature heat treatment [171]. On the other hand, the presence of polar sites on top of surface topography is essential to achieve superhydrophilicity. Immediately after laser texturing, oxide or hydroxide layers can form spontaneously on top of nanostructures and significantly increase the surface energy increasing hydrophilicity [100,172]. Several other chemical groups, such as acetoxy group (CH₃-C(=O)-O-R), carbonyl (-C(=O)-), carboxyl (-COOH) and nitrile (R-CN) can also increase hydrophilicity in nature. When those groups are attached to the nanostructured surface, surface behaves as

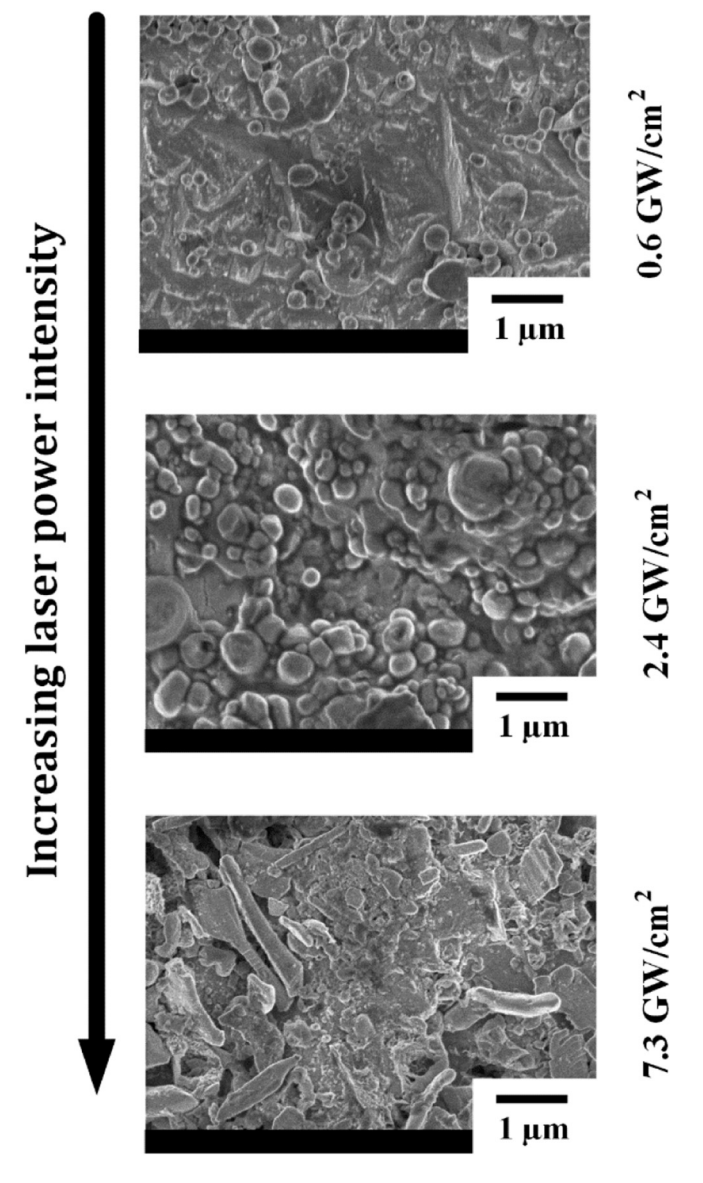


Fig. 7. Randomly distributed nanostructure with various shapes of protrusions, rods, cones, platelets, and pores on AlSI4130 steel with increasing laser power intensity. Adapted from [124] with permission of the Elsevier.

superhydrophilic due to a strong permanent dipole-dipole attraction force and van der Waals dispersion forces between molecules [173–175]. Boiling water treatment [172] and high-temperature heat treatment [100] are also used on a laser textured surface to achieve superhydrophilicity.

A complex combination of surface chemistry and surface micro/nanostructures affect the surface wettability. This complex combination is summarized in Fig. 8; by controlling the chemical groups on top of the surface nanostructure, wettability can be varied from superhydrophilicity to superhydrophobicity for the same underlying nanostructured surface. As depicted in the left column of Fig. 8, these are the typical top-down laser texturing methods to create LIPSS and hierarchical surface structures using nanosecond, picosecond, and femtosecond lasers. The middle column lists selected surface chemistry modification techniques applied after the laser texturing step. The right column represents the wettability scenario after the surface corresponding to each surface chemistry modification technique.

As shown in Fig. 8A(i) and 7A(ii), hierarchical structures are created on copper by a nanosecond pulsed laser [158]. Large scale (100 μ m) cross-hatch designs along with small scale (< 10 μ m) ablated debris

can be seen on this processed surface. LIPSS feature on Ti-6Al-4V [138] (Figs. 8B(iii) and 7B(iv)) and hierarchical structures on copper [154] (Figs. 8B(v) and 7B(vi)) can be created by a picosecond laser treatments. 10 µm structures arranged in micro-cone arrays and smaller, single micron to nanoscale structures that represent LIPSS [154] are both observed in the resulting surface. LIPSS on titanium [127] (Figs. 8C(vii) and 7C(viii)) and hierarchical structures on austenitic stainless steel [156] (Figs. 8C(ix) and 7C(x)) can be created by femtosecond laser treatments. The hierarchical structures also contain micro-scale crosshatch patterns covered with nano-scale LIPSS features. Generally, the size of the surface features trend with the time of the laser pulse. Larger surface features created by nanosecond lasers and smaller features created by pico- or femtosecond lasers. Combining a nanosecond and picosecond laser pulses were reported to fabricate hierarchical cross-hatch patterns on Ti-6Al-4V alloy [131], as shown in Figs. 8D(xi) and 7D (xii). Similarly, a nanosecond and femtosecond laser fabricated hierarchical cross-hatch patterns on Ti-6Al-4V alloy is shown in Figs. 8E(xiii) and 7E(xiv) [132].

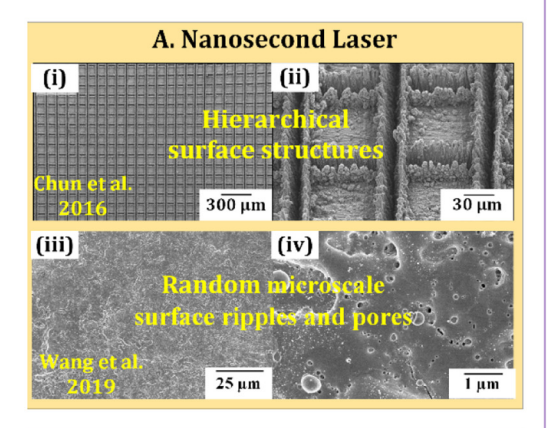
Among the surface chemistry modification techniques, extended exposure to ambient air is one of the most popular techniques to achieve superhydrophobicity. During the storage in air, laser textured aluminum surface absorbs airborne organic molecules that lead to superhydrophobicity [100], as shown in Fig. 8F. Adsorption of organic components on the nanostructured surface alters the surface chemistry with enrichment of -CH₂- and -CH₃ groups that contribute to superhydrophobicity [100]. Hydrophobic chemical treatment is also used to attach low energy long-chain fluoro-silane molecules with -CF₂- and -CF₃ groups leading to superhydrophobicity, as shown in Fig. 8G [76]. Low-temperature heat treatment process is also used before exposure to ambient air to increase the organic molecule adsorption, leading to superhydrophobicity (Fig. 8H) [171]. Chemical treatment with a hydrophilic functional group is one of the techniques to achieve superhydrophilicity where the hydrophilic group increases surface polarity to facilitate water affinity (Fig. 8I) [176]. Hightemperature heat treatment is often carried out to burn out the absorbed organic constituents to render superhydrophilicity (Fig. 8J) [100]. Boiling water treatment is also used post-laser texturing to enrich the surface micro-/nano-structures with polar oxide and hydroxide groups leading to superhydrophilicity (Fig. 8K) [172].

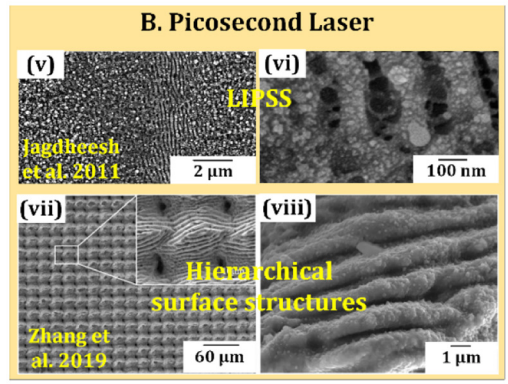
In summary, the relationship between surface chemistry modification methods (middle column) and corresponding surface wettability (right column) is row-wise; however, the relationship between laser texturing methods (left column) and surface chemistry modification methods (middle column) is not row-wise. Theoretically, any combination between the left column and the middle column is possible to achieve the desired wettability; however, only a few cases are presented in Fig. 8. A summary of chemistry modification methods and corresponding laser patterned surface structures for different materials is provided in Table 4. It also lists the characteristics of each combination of the two processes to achieve target extreme wettability. The following subsections detail the work done using the surface chemistry modification methods mentioned in Fig. 8.

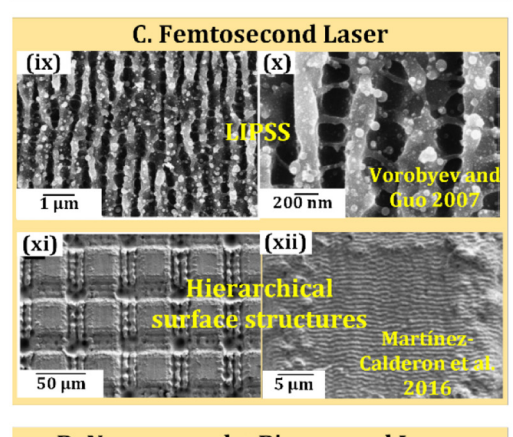
3.1. Long time exposure in air

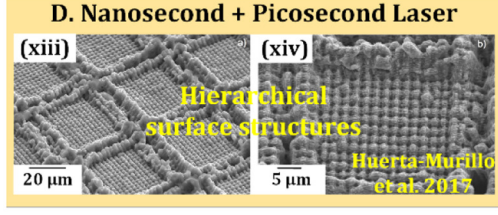
The wettability of laser-textured metal surfaces can change from hydrophilic to hydrophobic if the textured surface is exposed to air for extended periods of time. Similar transitions are observed for stainless steel [117,118,177,178], aluminum alloys [72,100,118,179], titanium alloys [117], copper [71], brass [71,157], nickel [209] and Inconel [180]. This wettability transition is also observed for micro/nanostructures generated by all three main categories of pulsed lasers, i.e., nanosecond [71,72,157,177–180], picosecond [100], and femtosecond [117,118]. This group of studies generally shows that surfaces are superhydrophilic, $\theta_{\rm W} < 30^{\circ}$, immediately after the laser texturing treatment. Within one week of exposure in air, the wettability changed to

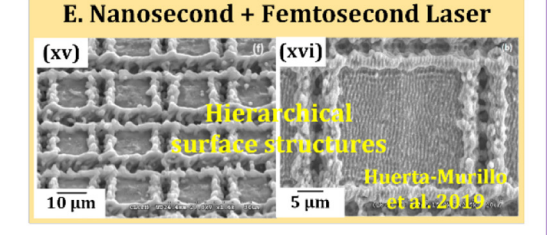
Laser Surface Texturing Methods

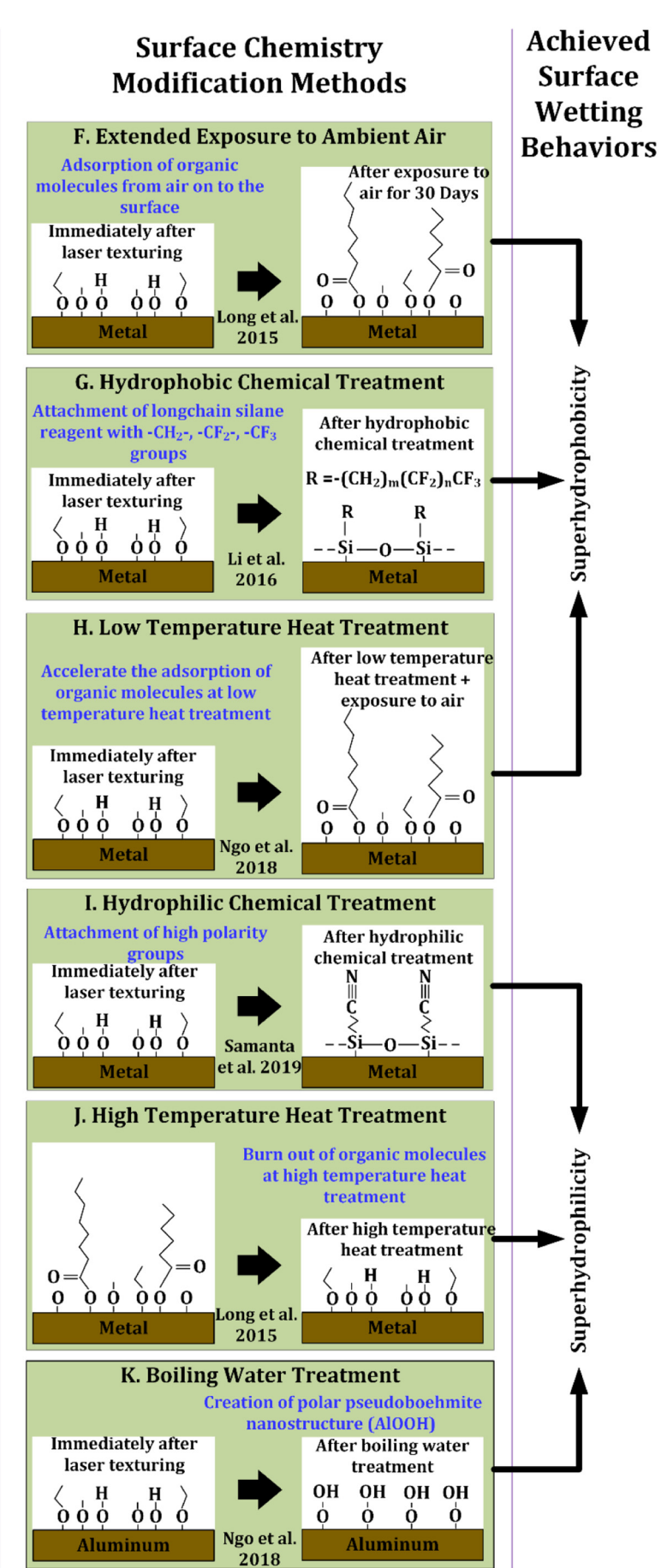












hydrophobic ($\theta_w \sim 90^\circ$), and within two weeks, the surfaces become superhydrophobic with $\theta_w > 150^{\circ}$ (Fig. 9a). The surfaces exhibit stable superhydrophobicity thereafter. $\theta_{Roll-off}$ and θ_{H} are reduced with exposure time, and the final value remains <10° after wettability is stabilized. Summary of θ_{W} , $\theta_{Roll-off}$ and θ_{H} can be found in Table 3 for different materials after exposure to air for a specific period of time. Researchers have studied the contributing factors to this wettability transition and generally concluded that the exposure to air does not change the micro/nanostructures. However, the surface is influenced by surface chemistry changes [100,117,118]. Different processing environments were also studied during laser texturing of AISI 304 stainless steel, including oxygen, air, carbon dioxide, nitrogen, and argon [126]. After that, textured samples were kept in sterile individual plastic bags filled with air for 7 days. It shows that surface textured in argon environment achieves $\theta_w=125^\circ$ whereas surfaces processed in oxygen, air, carbon dioxide, nitrogen had $\theta_w = 31^\circ$, 46° , 50° , and 83° , respectively after 7 days. Although the authors did not explain the chemical modification explicitly due to storage in air, their XPS study shows a significant amount of carbon carbon on the surface, indicating adventitious adsorption of organic or biomolecules during storage in sterile individual plastic bags. It indicated that laser processing environment could also influence the wettability transition rate.

Long et al. [100] did a thorough analysis of aluminum to identify the mechanism contributing to this wettability transition. Immediately after laser texturing, aluminum oxide surfaces are known to have many polar sites composed of unsaturated aluminum and oxygen atoms, which lead to an overall hydrophilic surface [181,182]. When the textured samples are kept in N₂, O₂, and CO₂ atmosphere, the surface remained as superhydrophilic, showing that these gasses do not cause the wettability transition of aluminum. However, the Earth's atmosphere consists of several categories of organic constituents, including long-chain hydrocarbons with carbonyl groups, carboxylic acids, and diol groups [183–185]. Long et al. [100] observed that separate surfaces kept in air and an atmosphere with volatile polar organics (4-Methyloctanoic acid) showed a significant transition of wettability (Fig. 9b) to superhydrophobicity within thirty or eight days respectively. XPS analysis shows that the amount of carbon on these surfaces (Fig. 9c) and the carbon to aluminum ratio (Fig. 9d) increased drastically over the same time periods. Further detail analysis of C 1s peak shows (Fig. 9e) that the textured aluminum surface stored in air has a high percentage of nonpolar C-C(H) bond, polar -C-O-, polar -C=O and polar -COO⁻ content which agrees with the functional groups expected to be present in the ambient air environment. This indicates that adsorbed organic compounds from likely to form a hydrophobic coating on the otherwise hydrophilic metal-oxide surface. We believe the presence of polar sites in both laser textured surface and organic constituents of the atmosphere works as a driving force for organic adsorption. The polar sites on textured aluminum interact favorably with the polar groups on volatile organic that are otherwise rich with alkyl groups (Fig. 9f). Adsorption reduces the surface polarity of aluminum oxide.

There are other theories to explain the surface chemistry change, including partial surface deoxidation on textured copper [71,158,169], and catalyzed decomposition of CO_2 into carbon with active magnetite

[117] for steel. Chun et al. [158] and Ta et al. [71] proposed partial surface deoxidation on textured copper for achieving superhydrophobicity for copper during exposure in air. During laser texturing, the textured surface consists of cupric oxide (CuO), which is hydrophilic in nature [169]. Chun reports the processed surface is superhydrophilic immediately after laser texturing. When the textured copper surface is exposed to ambient condition, partial deoxidation converts cupric oxide (CuO) into cuprous oxide (Cu₂O), increasing the ratio of Cu₂O to CuO over time. Cuprous oxide (Cu₂O) is reported to be hydrophobic [169]. Therefore, the deoxidation process could be responsible for a change of wettability. However, copper is known to be fully oxidized in the presence of air and is unlikely to be spontaneously reduced in an ambient environment. Kietzig et al. [117] proposed a theory based on the catalyzed decomposition of atmospheric CO₂ into carbon with active magnetite. CO₂ is a very stable molecule with significant barriers to activation, so any decomposition reaction would proceed very slowly if at all. Kietzig did report an accumulation of non-polar carbon on the textured steel surface, but it is likely to be from similar sources mentioned above rather than reduced carbon from CO₂.

Our review indicates that the most widely accepted theory of surface chemistry modification by exposing to ambient air is the adsorption of airborne organics with aliphatic groups [100]. There is no influence of CO_2 , O_2 , or N_2 in wettability transition. However, this air-exposure is not well controlled or reproducible; the wettability transition varies from location to location due to the disparity in concentration and composition of airborne species. It also takes a very long time for the wettability transition to occur, and the time required is material dependent with aluminum alloy, brass, and copper achieving stable superhydrophobicity within 10 days whereas steel, titanium alloy, and Inconel take more than 15 days [71,132,178–180].

3.2. Chemical treatment

Chemical treatments in the form of chemisorbed monolayers are well established as a method to alter surface wetting behaviors [108,163,186]. Laser textured metals can also be tuned to desired wettability conditions using this approach. For chemical treatments, silanes are one of the most widely applied materials because they offer direct modification with both superhydrophobic and superhydrophilic functionalities [125,145,187-189]. Silane surface treatment is typically achieved by coating the laser textured surface with a monolayer of functionalized silane reagent, thus inducing the change of chemical composition on the laser textured surface. Fluorinated groups with low binding energy such as -CF₂- and -CF₃ and alkyl (CH₂)_n groups on a nanostructured surface can reduce the surface energy and lead to superhydrophobicity. In contrast, due to their high polarity, attaching nitrile (-CN), carbonyl (-C(=0)-), and carboxyl (-COOH) groups, so a surface via silane chemistry creates significant shifts to hydrophilicity [190–193]. In the following paragraphs, we review chemical methods to achieve superhydrophobicity and superhydrophilicity.

In order to achieve hydrophobicity for laser textured metal alloys, researchers use chemical treatment after the laser texturing process [76,100,187,194]. Typical chemical formulae of these chemicals include

Fig. 8. Summary of combinations of typical top-down laser textured micro/nanoscale surface structures and surface chemistry modification methods led to wettability change. (A) (i, ii) Hierarchical surface structures in two different magnification generated on copper by nanosecond pulsed laser. Reproduced from [158] with permission from Elsevier. (iii, iv) Random nanoscale surface ripples and pores on AISI4130 steel after nanosecond laser texturing underwater. Reproduced from [124] with permission from Elsevier. (B) (v, vi) LIPSS in two different magnification generated by picosecond pulsed laser. Reproduced from [138] with permission from ACS. Hierarchical surface structures by picosecond pulsed laser (vii) microscale structures (C) (ix, x) LIPSS on top of microscale structures. Reproduced from [154] with permission from Elsevier. (C) (ix, x) LIPSS in two different magnification generated by femtosecond pulsed laser. Reproduced from [127] with permission from Elsevier. (xi, xii) Hierarchical surface structures by femtosecond pulsed laser with (xi) microscale structures and (xii) LIPSS on top of microscale structures. Reproduced from [156] with permission from Elsevier. (D) Hierarchical surface structure by hybrid laser process with (xiii) microscale surface structures by nanosecond laser and (xiv) LIPSS on top of microscale features generated by picosecond pulsed laser. Reproduced from [131] with permission from Elsevier. (E) Hierarchical surface structure by hybrid laser process with (xv) microscale surface structures by nanosecond laser and (xvi) LIPSS on top of microscale features generated by femtosecond pulsed laser. Reproduced from [132] with permission from Elsevier. (F) Mechanism of the organic molecule adsorption to change of surface chemistry when exposed to air for an extended period leading to superhydrophobicity. (G) Mechanism of change of surface chemistry during hydrophobic chemical treatment with fluorinated groups and alkyl groups leading to superhydrophobicity. (H) Mechanism of the change of s

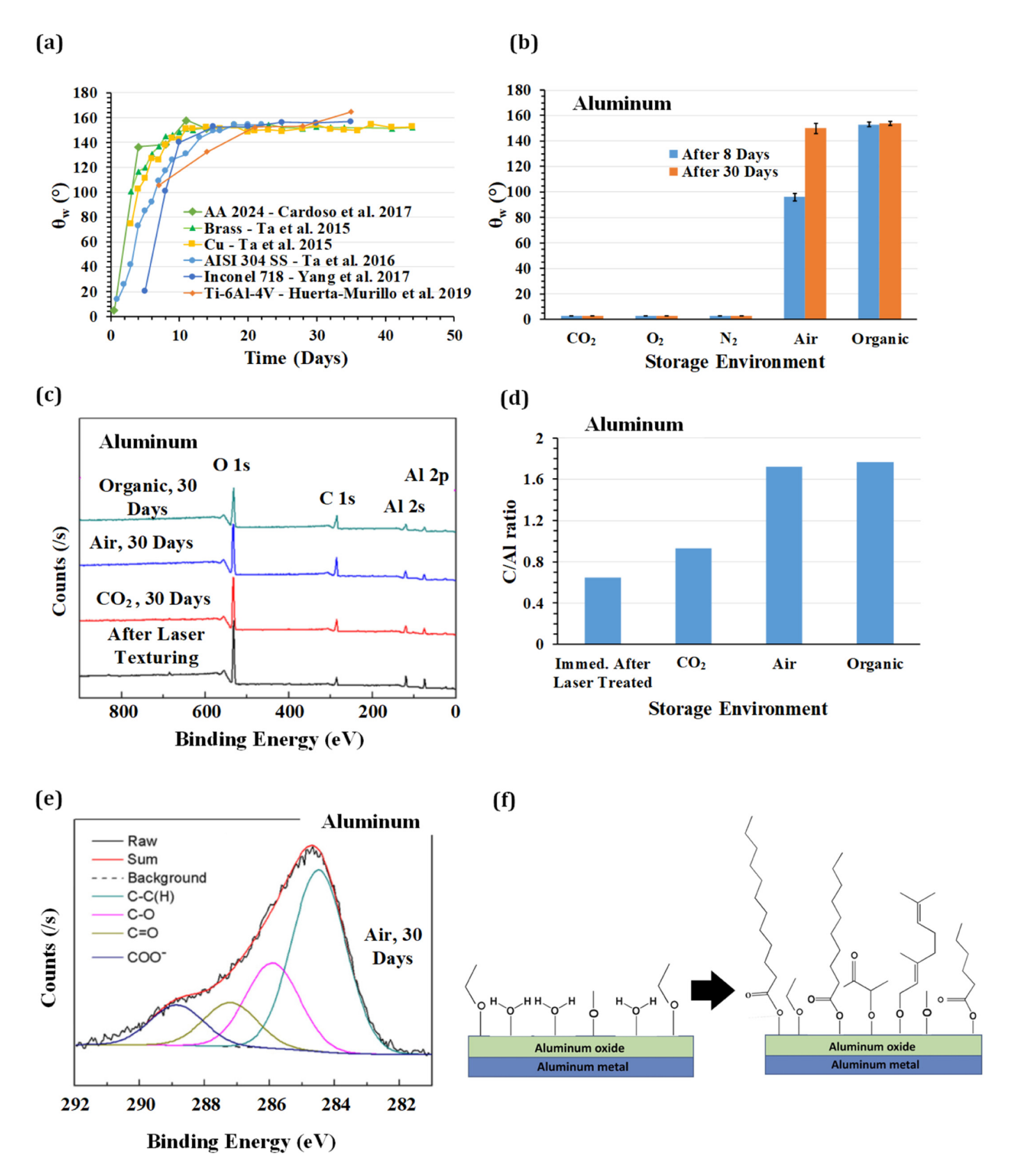


Fig. 9. Wettability transition by storing the laser textured metal surface in air for a long time: (a) change of θ_w with exposure time in air for different metal alloys, plotted by the author from data reported in [71,132,178–180] with permission from Elsevier and RSC; (b) change of θ when the textured aluminum alloy is kept in different environment, plotted by the author from data reported in [100] with permission from Elsevier; (c) XPS spectra over the binding energy range from 0 to 900 eV for different laser textured aluminum samples kept in different environments. Reproduced from [100] with permission from Elsevier. (d) Change in C/Al ratio when laser textured aluminum samples kept in different environments, plotted by the author from data reported in [100] with permission from Elsevier. (e) C 1s spectra on the laser textured aluminum surface that is kept in air for different metal alloys, plotted by the author from data reported in [100] with permission from Elsevier. (e) C 1s spectra on the laser textured aluminum. Reproduced from [100] with permission from Elsevier.

Table 3Wettability measurement parameters for laser textured materials after exposure to air.

Material	Exposure days	θ _w (°)	$\theta_{Roll-off}$ (°)	θ _H (°)	Reference
SS304	18- 22	155	N.R. ^a	~4	[178]
Aluminum	15	158	3- 5	<5	[72]
Copper	44	152	~2.0	3-4	[71]
Brass	44	153	~2.9	3-4	[71,157]
Inconel	35	156.8	6.5	N.R.	[180]

^a N.R. = not reported.

fluoro-silanes expressed as X¹SiR¹ [195] (where X¹ stands for chlorine or a C1-C6 -alkoxy group and R1 is a C8-C20 -fluoro-substituted alkyl group $[(CH_2)_2C_nF_{2n+1}])$ or alkyl groups which are $[C_nH_{2n+1}]$. Other chemicals used can be expressed as Y¹R¹, where Y¹ stands for thiol (-SH), carboxyl (-COOH), etc. In those chemical reagents, X¹ and Y¹ serve as a reactive group that reacts with the laser textured Surface and gets the molecules attached to the textured surface. In contrast, the R¹ group serves as the functional group to alter the surface energy/wettability [195]. Researchers routinely utilize chemical vapor deposition (CVD) [125,138], vacuum oven treatment [76,145], or immersion in dilute ethanolic solutions of these surface modifying agents [188,189] to attach them chemically to laser-textured surfaces (Fig. 10a). Chemical treatment processes achieve superhydrophobic wetting conditions for a wide range of engineering metal alloys including steel [98,125,138,145,187,189,196], aluminum alloy [100,187,194], titanium alloy [76,138,187,197,198], copper [155,211], and zinc [199]. Long-chain alkanethiols are also used as self-assembled monolayers on coinage metals such as palladium [200,201], gold, and silver [202–207], to create a passivating and wetting resistant surface.

Kam et al. [125] applied tridecafluoro-1,1,2,2,-tetrahydrooctyl-1-trichlorosilane $[CF_3(CF_2)_5(CH_2)_2SiCl_3]$ by the chemical vapor deposition

(CVD) on top of laser-fabricated micro-conical structure on AlSI 316L to make it superhydrophobic. Wu et al. [145] applied 97% Trichloro (1H, 1H, 2H, 2H-perfluorooctyl) silane [CF $_3$ (CF $_2$) $_5$ (CH $_2$) $_2$ SiCl $_3$] by CVD process on femtosecond laser textured LIPSS on stainless steels to achieve superhydrophobicity. Pendurthi et al. [187] applied heptadecafluoro-1,1,2,2-tetrahydrodecyl trichlorosilane [CF $_3$ (CF $_2$) $_7$ (CH $_2$) $_2$ SiCl $_3$] after the laser texturing process on the titanium, aluminum, several stainless steels to make them superhydrophobic. Through XPS analysis, they showed the presence of fluorinated groups (-CF $_2$ - and -CF $_3$) with a low binding energy that contributed to the superhydrophobicity, as shown in Fig. 10b.

It is well known that a surface needs to be polar to exhibit superhydrophilic wetting. Researchers also use chemical treatments to enhance hydrophilicity, such as those with nitrile (-CN), carbonyl (-C (=0)-), and carboxyl (-COOH) functional groups. These groups are known to be highly polar due to the presence of highly electronegative nitrogen and oxygen atom in the chemical structure. As electronegativity of nitrogen and oxygen is very high, they attract electron density from the covalent bond, inducing a net dipole moment. Nitrile (-CN), carbonyl (-C(=O)-), and carboxyl (-COOH) groups, therefore, can participate in significant dipole-dipole interactions with water as well as van der Waals dispersion forces [173-175]. The authors' research group utilized immersion treatment in dilute solutions of hydrophilic silanes in ethanol solution [176] for aluminum and titanium alloys to chemically attach silane reagents on the laser textured surfaces as shown in Fig. 11a. As mentioned earlier, during the process, the hydrophilic functional groups are chemically attached to the surface and contribute towards a polar surface. In this case, the textured surface, as shown in Fig. 11b, had nitrile (-CN) group attached on the surface as proved by XPS analysis (Fig. 11c) that contributed to superhydrophilicity. The processed surface shows stable

 Table 4

 Summary of different characteristics related to the combination of top-down laser patterned surface structures and corresponding chemistry modification methods to achieve extreme wetting conditions.

			Characteristics								
			Mechanism of chemistry modification	Controllability of chemistry modification	Time required for chemistry modification	Stability of wettability	Stability of Cassi-Baxter state	Metals and alloys	Laser type		
			xxx	x	x	xx	xx	Steel [118], Al alloy [118] Cu [208]	Femtosecond	LIPSS	
		Extended exposure to	xxx	х	x	xx	xxx	Steel [117,156], Ti alloy [117]	Femtosecond	Hierarchical	
		ambient air	xxx	x	x	xx	xxx	Al alloy [100] Ni [209]	Picosecond	surface	
	ity		xxx	х	х	xx	xxx	Steel [177,178,210], Al alloy [72,129], Cu [71], Brass [157], Inconel [180]	Nanosecond	structures	
s	bje		XX	xxx	xxx	x	x	Steel [145]	Femtosecond		
ethod	ropho		xx	xxx	xxx	x	x	Steel [138], Ti alloy [138,197], Cu [101]	Picosecond	LIPSS	
m mo	Superhydrophobicity	Hydrophobic chemical treatment	xx	xxx	xxx	xxx	xxx	Steel [125,145,189], Ti [76,188], Cu [45,155]	Femtosecond	Hierarchical surface structures	ъ
ificati	Sup		xx	xxx	xxx	xxx	xxx	Steel [196], Al [100], Ti alloy [197,198]	Picosecond		ucture ty
pou			xx	xxx	xxx	xxx	xxx	Steel [98], Zn [199] Cu [211]	Nanosecond		
Surface chemistry modification methods		Low temperature heat treatment	xx	x	xx	xx	xxx	Steel [78,212,213], Al & Al alloy [171,172,212], Cu & Cu alloy [158,171,212], Ti & Ti alloy [171,212,214], Mg alloy [23]	Nanosecond		Surface structure type
Su	icity	Hydrophilic chemical treatment	xx	xxx	xxx	xx	N/A	Al [176], Ti alloy [176]	Nanosecond	Hierarchical surface structures	
	Superhydrophilicity	High-temperature heat treatment	xx	x	xx	x	N/A	Al [100]	Picosecond		
	Supe	Boiling water treatment	x	xx	xx	xx	N/A	Al [172]	Nanosecond		
		Very good / St	ufficient understand	ling xx	Moderate /	Partial understar	nding	x Poor / Limited unde	erstanding		

Table 5Heat treatment conditions of different materials for achieving specific wetting conditions.

Material	Heat treatment condition	Wettability	References
Ti and Ti alloy	100 °C for 24 h	Superhydrophobicity	[171,212,214]
	200 °C-300 °C for 2 h	$\theta_{\rm w} > 160^{\circ}, \theta_{\rm roll-off} < 5^{\circ}$	
Stainless steel	100 °C-150 °C for 24 h	Superhydrophobicity	[78,212,213]
		$\theta_{\rm w} > 160^{\circ}, \theta_{\rm roll-off} < 7^{\circ}$	
Mg alloy	160 °C for 1 h	Superhydrophobicity	[23]
		$\theta_{\rm w} = 158^{\circ} \theta_{\rm roll-off} = \text{N.R.}$	
Al and Al alloy	100 °C for 24 h	Superhydrophobicity	[171,172,212]
•	200 °C for 2 h	$\theta_{\rm w} > 160^{\circ}, \theta_{\rm roll-off} < 5^{\circ}$	
	250 °C for 20 min	Superhydrophilicity	[100]
		$\theta_{\rm w} < 10^{\circ}$	
Cu and Cu alloy	100 °C for 24 h	Superhydrophobicity	[158,171,212]
Į.	200 °C for 2 h	$\theta_{\rm w} > 160^{\circ}, \theta_{\rm roll-off} < 8^{\circ}$	
	350 °C for 20 min	Superhydrophilicity	[100]
		$\theta_{\rm w} < 10^{\circ}$. ,

superhydrophilicity with $\theta_w=0^\circ$ for a tested period of 30 days as shown in Fig. 11d. When the water droplet comes in contact with the processed surface, it immediately spread on the surface as shown in Fig. 11e.

The silane reagent with chlorine as the reactive group produces an etching effect during the chemical treatment [124]. These chlorine atoms reacted with the metal substrate during the chemical treatment and dissolved in the chemical solution as metal chloride, which enhances the surface structuring process [124,133]. The silane molecule also gets itself attached to the surface structures simultaneously during the process as well.

Chemical treatment provides additional pathways to modify surface wettability by controlling the surface functional groups. Low energy functional groups like -CH₂-, -CH₃, -CF₂- and -CF₃ leads to superhydrophobicity, whereas polar groups like -CN contribute towards superhydrophilicity. The mechanism of attachment of functional groups on the laser textured surface and the effect of their length on the final wettability is not explained systematically in existing works, providing an opportunity for future studies. Further, only a few hydrophilic functional groups are investigated as monolayers on these surfaces for

Table 6Comparison of corrosion resistance of different laser textured metal alloys [98,222,225].

Material	SS 316L	S45C steel	AA7075
Laser treatment	Nanosecond	Nanosecond	Nanosecond
[structure type]	[microcolumns]	[spot array]	[spot array]
Chemistry modification	Fluoropolymer	Fluoropolymer	Fluoropolymer
$\theta_{\rm w}$ (base/treated)	95°/155°	70.6°/161.5°	70.6°/155.6°
$\theta_{Roll-off}$ (base/treated)	Pinned/3°	Pinned/N.R.	Pinned/3.8°
E _{corr} (mV) (base material)	292.4	480	714
E_{corr} (mV) (treated)	169.9	250	524
I _{corr} (Acm ⁻²) (base material)	5.01×10^{-7}	5.97×10^{-6}	4.96×10^{-6}
I _{corr} (Acm ⁻²) (treated)	3.16×10^{-9}	1.16×10^{-7}	8.87×10^{-8}

achieving superhydrophilicity, and these are studied on a similarly limited number of metal alloys [176]. Other metal/metal alloys and hydrophilic chemicals need to be investigated for the broad application of this process.

3.3. Heat treatment

The surface wettability of the laser textured metal surface is also influenced by heat treatment. After the heat treatment, the laser textured metals/metal alloys were kept in air, and their wettability changes rapidly. Depending on the heat treatment temperature, wettability can vary from hydrophobicity [78,158,171,172,214,215] to superhydrophilicity [100]. Low-temperature annealing after the laser texturing process led to superhydrophobicity, whereas high-temperature annealing led to superhydrophilicity. After the heat treatment, the surface micro/nanostructure remained the same [100,171]. Therefore the wettability transition occurred due to surface chemistry change during or after the heat treatment process [100,171]. Annealing conditions for different materials are listed in Table 5 for achieving superhydrophobicity and superhydrophilicity.

Ngo and Chun [171] performed a comprehensive analysis of lowtemperature annealing after the laser texturing process for aluminum, copper, and titanium to find out the mechanism of wettability transition. The heat treatment process is schematically shown in Fig. 12a. After the heat treatment, the treated surfaces were stored in air. Controlling the heat treatment temperature influences the transition period to achieve superhydrophobicity, as shown in Fig. 12b. This annealing process is also material dependent, as shown in Fig. 12c. Titanium reached superhydrophobicity over a shorter time than aluminum and copper. It has been hypothesized that the annealing process accelerated the organic absorption from the atmosphere when it was kept in the air after the treatment. However, the analysis has not been carried out systematically to support the hypothesis. FT-IR measurement showed strong -OH functional group on the laser textured surface whereas after the heat treatment and exposure to ambient air for several hours, -OH group disappeared and hydrophobic groups (-CH₃ and -CH₂-) can be observed on the treated surface for all three materials

Table 7Comparison of abrasion resistance of different laser textured metal alloys [188,226,227].

Material	Titanium	SS 12X18H10T	SS X6Cr17	SS X6Cr17
Pre-laser treatment	None	None	None	Carburizing
Laser treatment [structure type]	Femtosecond [microcolumns]	Femtosecond [microtrenches]	Nanosecond [microtrenches]	Nanosecond [microtrenches]
Chemistry modification	Fluoropolymer	Fluoropolymer	Fluoropolymer	Fluoropolymer
Standard of abrasion test	None	ASTM F735	ISO 11998:2006	ISO 11998:2006
Abrasion test time/cycles	200 cycles	2 h	300 cycles	300 cycles
θ _w (before/after)	165°/120°	170.9°/155.0°	171°/110°	172°/146.0°
$\theta_{Roll-off}$ (before/after)	6.5°/Pinned	1°/14.7°	N.R.	N.R.
θ _H (before/after)	7°/> 50°	N.R.	N.R.	N.R.

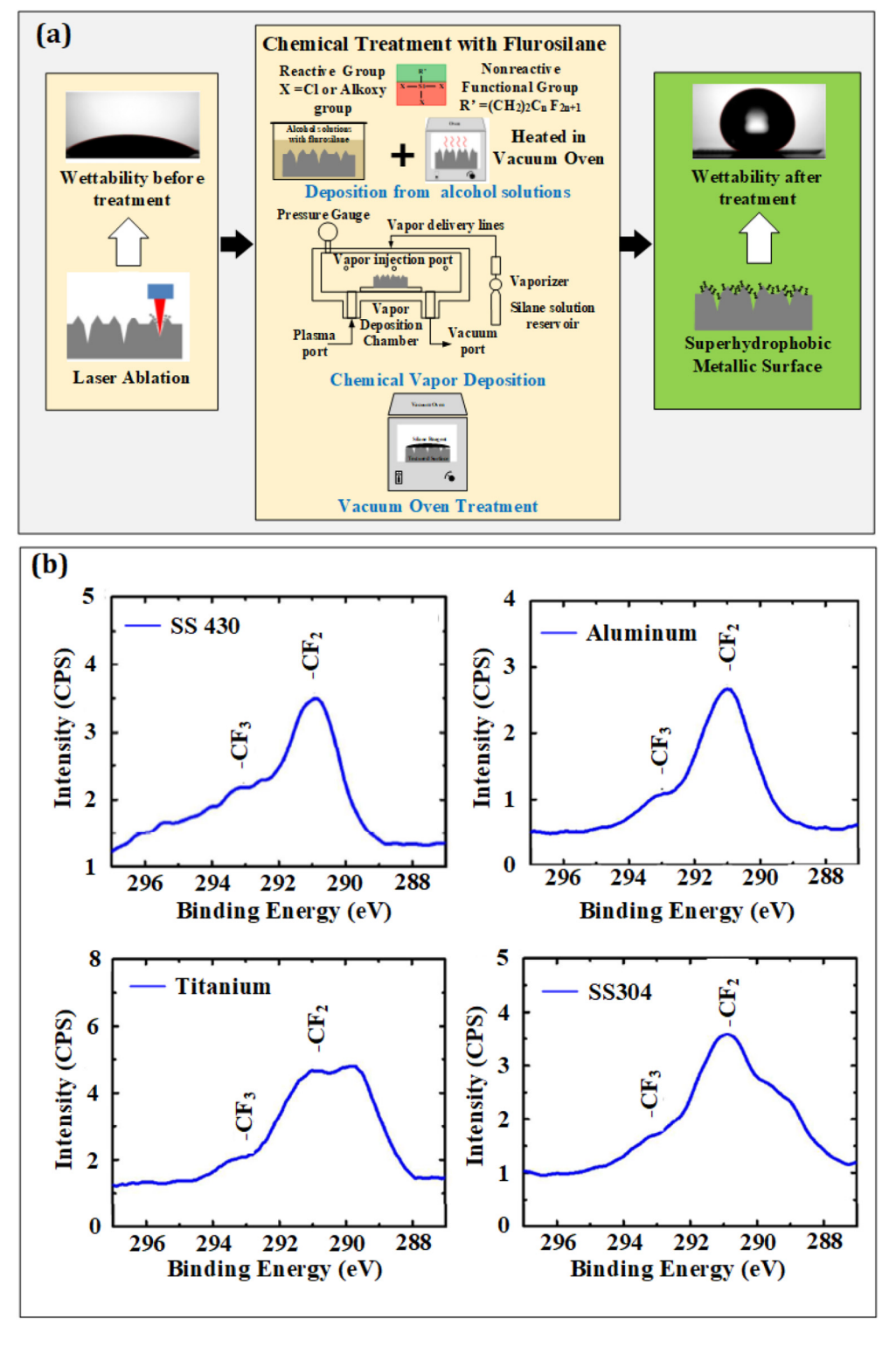


Fig. 10. Superhydrophobicity on laser textured metal surface by chemical treatment: (a) Schematic representation of chemical treatment by immersion in silane-ethanol mixer solution, chemical vapor deposition (CVD), or vacuum oven treatment and subsequent wettability change; (b) XPS spectrum on fluoro-silane treated superhydrophobic metal alloys showing the existence of –CF₂- and –CF₃ on the treated surface. Reproduced from [187] with permission from ACS.

(Fig. 12d, e and f) [171,172]. However, no FT-IR measurement was carried out immediately after heat treatment to understand what chemical transformation happens due to heat treatment alone. More likely, the heat treatment drives off -OH functional group from the laser textured surface and accelerates the oxidation of the surface. The heat treatment process most likely opens active surface sites for adsorption of organic species by removing water and makes more terminal oxide groups.

Those terminal oxide groups intensify the adsorption of the polar functional groups of the hydrophobic organic species when heat-treated specimens are stored in air. These two chemical events presumably help to accelerate the organic molecule absorption from ambient air. This proposed mechanism is supported by the FT-IR results, as in Fig. 12d–f. There is an increase in carbon content with strong -CH₂-and -CH₃ peaks for all three materials. It indicates that the long-chain

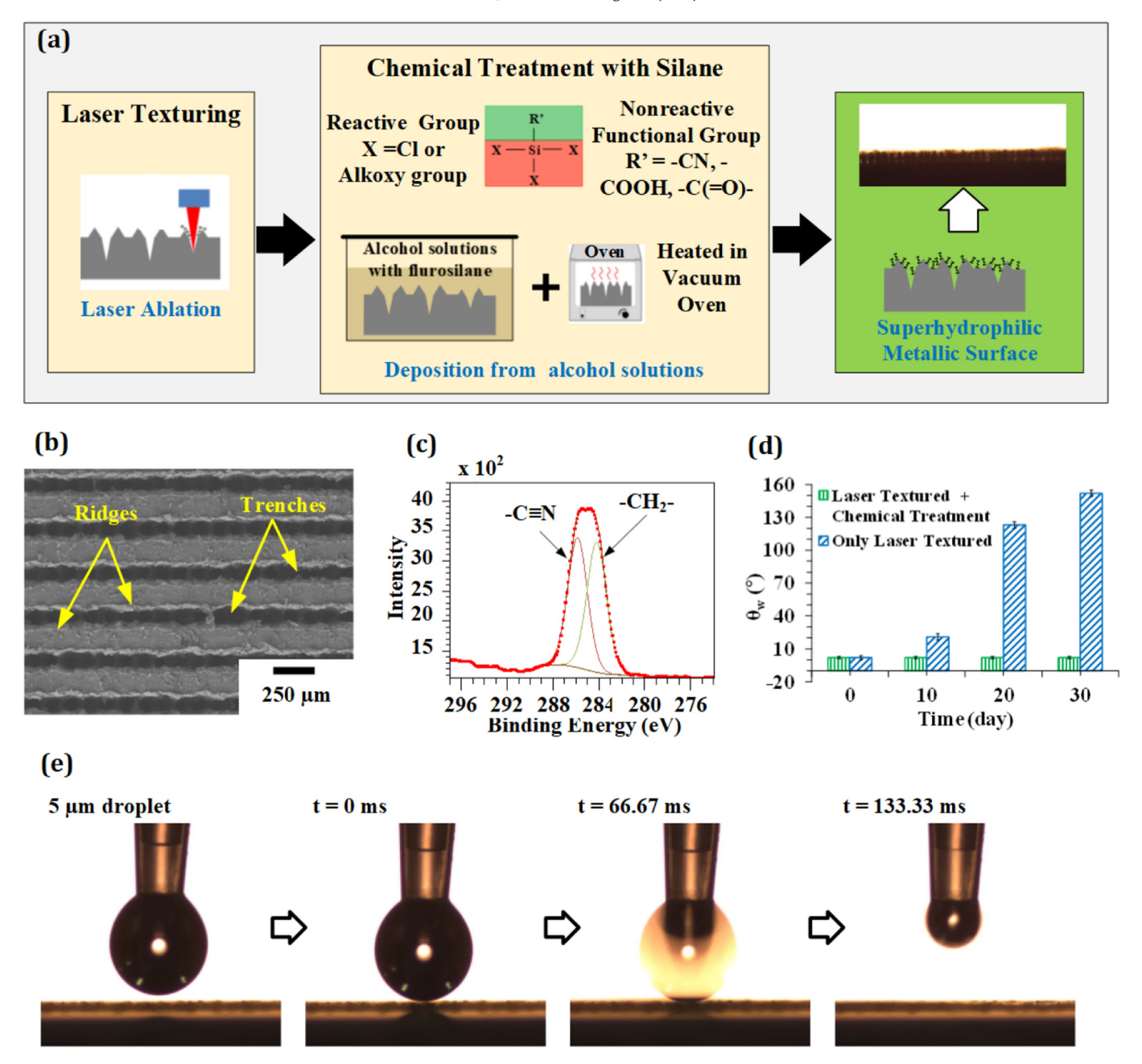


Fig. 11. Superhydrophilicity on laser textured metal surface by chemical treatment: (a) Schematic representation of chemical treatment by immersion in silane-ethanol mixer solution and subsequent wettability change; (b) SEM images of the treated aluminum surface; (c) XPS spectrum on silane treated superhydrophilic aluminum alloy showing the existence of –CN on the treated surface that contributed to superhydrophilicity; (d) stability of hydrophilic wettability on the only laser-treated aluminum and laser + chemical treated aluminum in air; (e) interaction of water droplet with the processed surface showing superhydrophilicity. Reproduced from [176] with permission from Elsevier.

hydrocarbon present in organic molecules in ambient air are adsorbed on the heat-treated surface. Those hydrophobic hydrocarbon groups reduce the surface energy of the heat-treated surface leading to superhydrophobicity. There is one additional theory to explain the wettability transition for laser textured copper after heat treatment. CuO nanoparticles trends to slowly convert to Cu₂O by reduction upon heating over 150 °C [216]. As mentioned earlier, CuO and Cu₂O are known to hydrophilic and hydrophobic, respectively [169]. After the heat treatment of laser textured copper at 200 °C for 2 h, x-ray diffraction results show an increase in the ratio of Cu₂O to CuO [158,171]. This confirms the transition of CuO to Cu₂O on the surface layer.

On the other hand, high-temperature annealing (250 °C for aluminum and 350 °C for copper) leads to transition of wettability from superhydrophobicity to superhydrophilicity [100,169,217]. There was no change of morphology on the pre- and post-heat treatment

processed surface [100]. Therefore, this transition was also due to the change in surface chemistry. The carbon content reduced on the surface after the high-temperature heat treatment, which implies that some of the organic molecules could not sustain high temperatures. Some of them were converted into $\rm CO_2$ and removed from the surface resulting in a lower C/metal ratio [100]. This suggests an increase of polar functional groups after the heat treatment, which leads to superhydrophilicity. However, the authors suspect that this transition is not sustainable. After exposing this to ambient air for a few days, it will presumably regain superhydrophobicity due to organic molecule adsorption.

Although there is significant research carried out on low temperature heat treatment to achieve superhydrophobicity, the underlying mechanism of wettability change is not well established. Although it has been claimed that the airborne organic molecule adsorption is

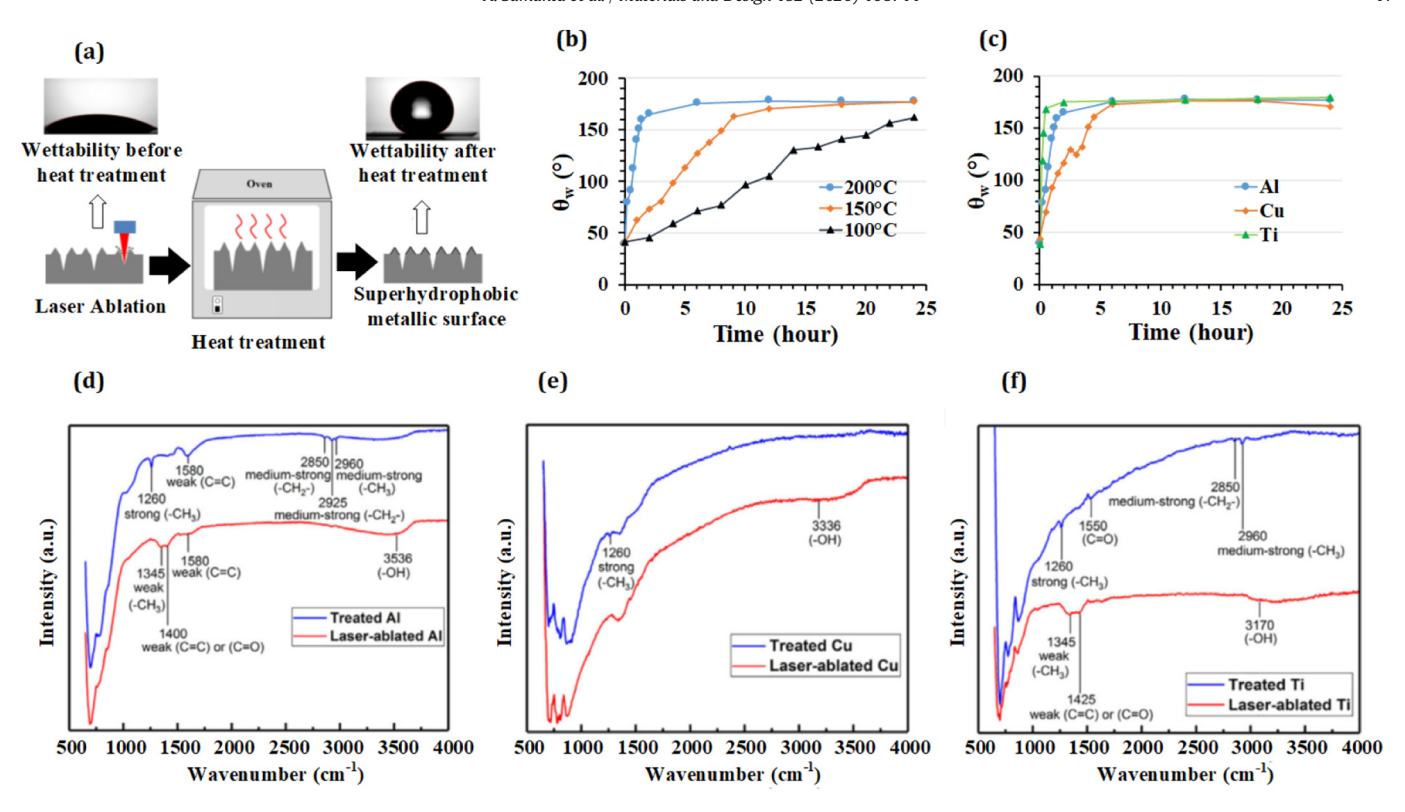


Fig. 12. Stable superhydrophobicity on laser textured metals by heat treatment: (a) Schematic representation of the heat treatment process. Reproduced from [171] with permission from Elsevier. (b) Change of θ_w with exposure time in air for aluminum heat treated at different temperatures, plotted by the authors using data from [171] with permission from Elsevier. (c) Change of θ_w with exposure time in air for aluminum, copper, and titanium heat-treated at 200 °C, plotted by the authors using data from [171] with permission from Elsevier. (d, e, f) Fourier transform infrared spectroscopy (FT-IR) comparison of untreated, laser-textured, heat-treated aluminum, copper, and titanium respectively, Reproduced from [171] with permission from Elsevier.

accelerated after the low-temperature heat treatment [171], systematic analysis has not been carried out. The textured metal should be kept in $\mathrm{CO_2}$, $\mathrm{O_2}$, and $\mathrm{N_2}$ atmosphere after heat treatment to investigate whether these components of the atmosphere has any influence on wettability change. Research on high-temperature heat treatment to achieve superhydrophilicity is limited to a few metals [100]. This process should be applied to other metals/metal alloys for wide acceptance of the processing mechanism. At the same time, high-temperature heat treatment might lead to some recrystallization and grain orientation change of the substrate metals, which might have an effect on wettability transition as well.

3.4. Boiling water treatment

Boiling water treatment after the laser texturing step resulted in prolonged superhydrophilicity for aluminum [172]. Ngo et al. [172] demonstrated that boiling water treatment on laser textured aluminum could produce stable superhydrophilicity for 60 days of testing by controlling the micro/nanostructure and surface chemistry. As demonstrated in Fig. 13a, the laser textured aluminum is treated with boiling water for 10 min to 120 min, and the samples show a $\theta_{\rm w}$ of ~0°. The processed sample can retain its superhydrophilicity for two months, as shown in Fig. 13c [172]. Longer boiling treatment provides better stability of surface superhydrophilicity on a non-textured surface, but the textured surfaces that are boiled for 10 or 120 min do not lose the hydrophilic property even after 60 days. A water droplet of 1 μ L volume can completely spread on the processed surface within 0.5 s for the sample treated for 120 min and 1.5 s for the sample treated for 10 min.

When the laser textured aluminum surface is treated with boiling water, a pseudoboehmite nanostructure is generated as the boiling water reacts with the aluminum [218], as expressed in eq. 4. After the boiling water treatment, the surface nanostructure changes due to the appearance of new pseudoboehmite (AlOOH) nanostructure Fig. 13b. At the same time, the surface chemistry was also modified significantly. More Al_2O_3 peaks along with new AlOOH were observed in the XRD study, as shown in Fig. 13d. Fourier transform infrared spectroscopy (FT-IR) further confirmed the appearance of new chemistry and pseudoboehmite microstructure appearance, as shown in Fig. 13e. The intensity of the -OH group is increased after boiling water treatment compared to only laser textured aluminum surface. AlOOH and Al_2O_3 surface chemistry and microstructures are well-known to have strong polar properties, which lead to an overall stable superhydrophilic surface.

Boiling water treatment is an exciting and straightforward avenue to achieve superhydrophilicity; however, this process is only explored on aluminum. Moreover, the mechanism, as explained, cannot be extrapolated to other materials. It is expected that other metal and metal alloys will be explored using this process to achieve superhydrophilicity in future. It is also worth investigating whether this process has any detrimental effect on specific metal alloys.

3.5. Discussion on durability of laser textured surface with chemistry modification

Wettability of a laser textured surfaces can degrade when they are exposed to a harsh environment through mechanical abrasion and chemical corrosion. Long-term durability and mechanical wear robustness are essential for large scale acceptance of laser-based surface texturing in industrial and commercial applications [219]. There have been few literature reviews discussing the durability and stability of

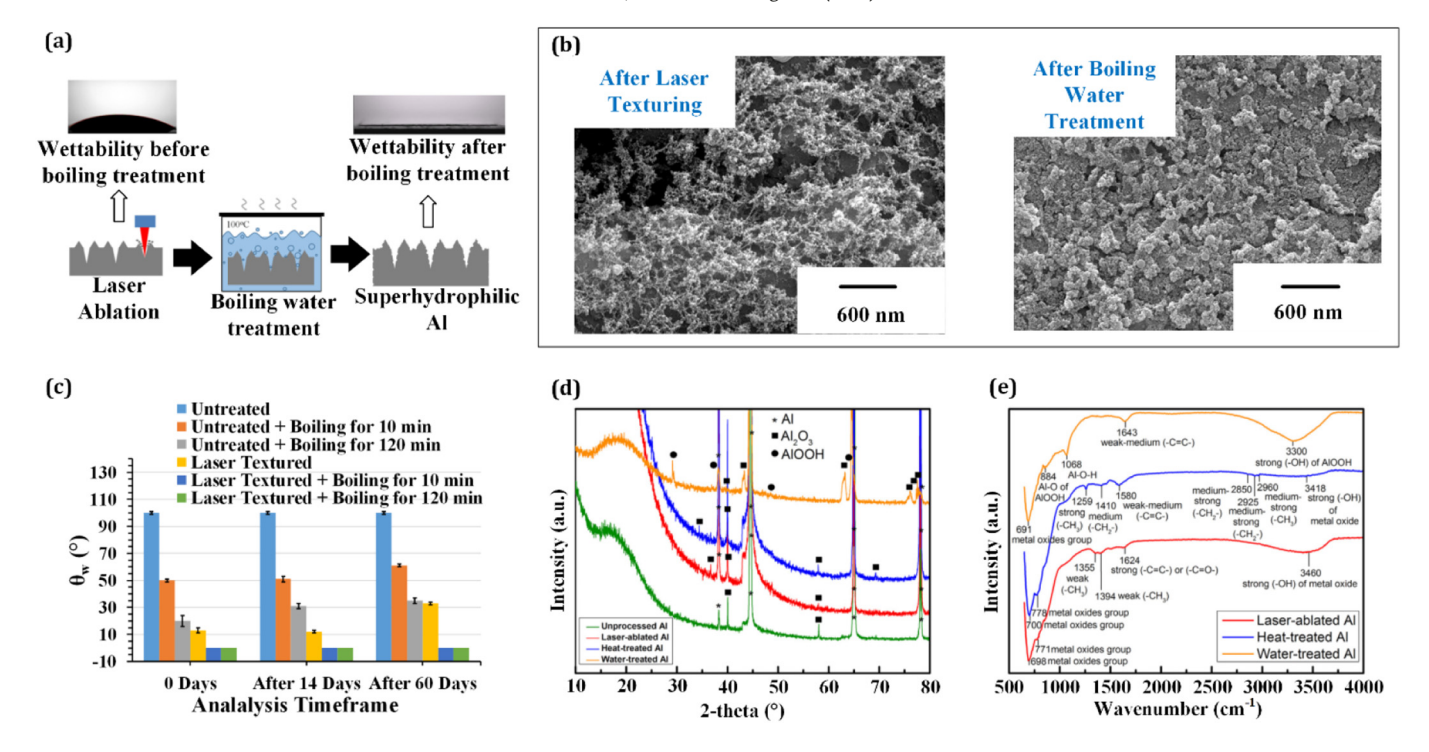


Fig. 13. Stable superhydrophilicity on laser textured aluminum by boiling water treatment: (a) schematic representation of boiling water treatment process. Reproduced from [172] with permission from Elsevier. (b) Difference in microstructure after the boiling water treatment. Reproduced from [172] with permission from Elsevier. (c) Wettability and stability of flat and laser-ablated aluminum with and without boiling water treatment, plotted by the authors using data from [172] with permission from Elsevier. (d) XRD comparison on untreated aluminum, laser-textured aluminum, heat-treated aluminum, and boiling-water-treated aluminum. Reproduced from [172] with permission from Elsevier. (e) Fourier transform infrared spectroscopy (FT-IR) comparison of laser-textured aluminum, heat-treated aluminum, and boiling-water-treated aluminum. Reproduced from [172] with permission from Elsevier.

nanostructured superhydrophobic surfaces in a harsh environment [107,220]. In this section, the focus will be only on the durability of laser texturing and chemical modification to corrosion and mechanical abrasion.

3.5.1. Corrosion resistance

Non-wetting behavior of surfaces often results in reduced corrosion rate of metals as it limits the interactions between surface and corrosive species in water [221]. Retention of corrosion resistance prolongs the lifecycle of the surface in a harsh environment. Therefore, it is very important to study the corrosion resistance of laser textured metal surfaces to retain surface features and surface chemistry for longer exposure time in a corrosive environment. There have been several corrosion studies on laser textured steel [98,210,222,223] and aluminum alloy [224,225] substrates.

Laser textured and fluorosilane treated metal alloys maintain superhydrophobicity in strong acidic (pH = 1), alkaline (pH = 13-14), and 3.5% NaCl solutions over a period of 24 h [98,225] as shown in Fig. 14a. However, strong acid and alkaline solution start to affect the wettability after 6 h, and slowly θ_w decreases, and $\theta_{Roll-off}$ increases over time. For AA7075, θ_w reduces to 145° after 5 and 8 days in acidic and alkaline solution, respectively [225]. Tafel polarization curves in Fig. 14b clearly shows the importance of the surface chemistry modification process after the laser texturing to have better corrosion resistance. The laser and fluorosilane treated surfaces have better anticorrosion capability in 3.5% NaCl aqueous than untreated and only laser-textured surfaces for stainless steel, AA7075, and aluminum [98,210,222–225]. It has higher corrosion potential and lower corrosion current compared to untreated and only laser-textured surfaces. The improvement of corrosion resistance by laser texturing and fluoropolymer treatment is summarized in Table 6. C-F bonds in fluorosilane surface chemistry are known to have strong chemical inertness and low surface energy, which can repel corrosive medium and prevent electron transfer from and into the substrate. Additionally, due to surface structure, air is trapped between a corrosive medium and substrate, as shown in Fig. 14c providing an effective barrier to avert corrosive media to chemically react with the substrate. The laser textured and fluorosilane treated 316L stainless steel also shows excellent durability to retain its corrosion resistance after one week of immersion in 3.5% NaCl aqueous solution, as shown in Fig. 14d. The corrosion potential and corrosion current did not change much after long time storage in saline solution. Ma et al. [222] show excellent healability for S45C steel even it lost its superhydrophobicity in 3.5% NaCl aqueous solution by further fluorosilane treatment. The above studies show that the chemical modification process after laser texturing provides excellent chemical stability and corrosion durability. However, most of these studies only consider fluorosilane treatment as a chemistry modification process and have not researched the other surface chemistry modification methods for comparison.

3.5.2. Abrasion resistance

Researchers have studied abrasion resistance of laser textured superhydrophobic metal surface chemically treated with fluorinated groups [188,226,227]. Steele et al. [188] selected titanium as substrate material as it inherently possesses outstanding mechanical durability. They textured it using a femtosecond laser followed by fluoropolymer coating. The abrasion test was performed with pressure conditions ranging from 108.4 to 433.7 kPa. θ_{w} reduces faster when higher pressure was applied. After 200 abrasion cycles, the surface features were destroyed. It was also observed that $\theta_{Roll\text{-}off}$ and θ_H degraded at a very fast rate within the first 10 cycles. Fatigue caused by repeated plowing by the abradant contributed as the primary mechanism of the abrasive wear. Secondly, the small particles separated from abradant during the test caused damage on the laser textured surface structures. Emelyanenko et al. [226] textured stainless steel with a femtosecond laser followed by fluorosilane coating and performed oscillating sand abrasion test according to ASTM F735 standard. After 2 h of abrasion test, the $\theta_{\rm W}$ deteriorated from 170.9 \pm 2.2 to 155.0 \pm 1.2° and $\theta_{\rm Roll-off}$

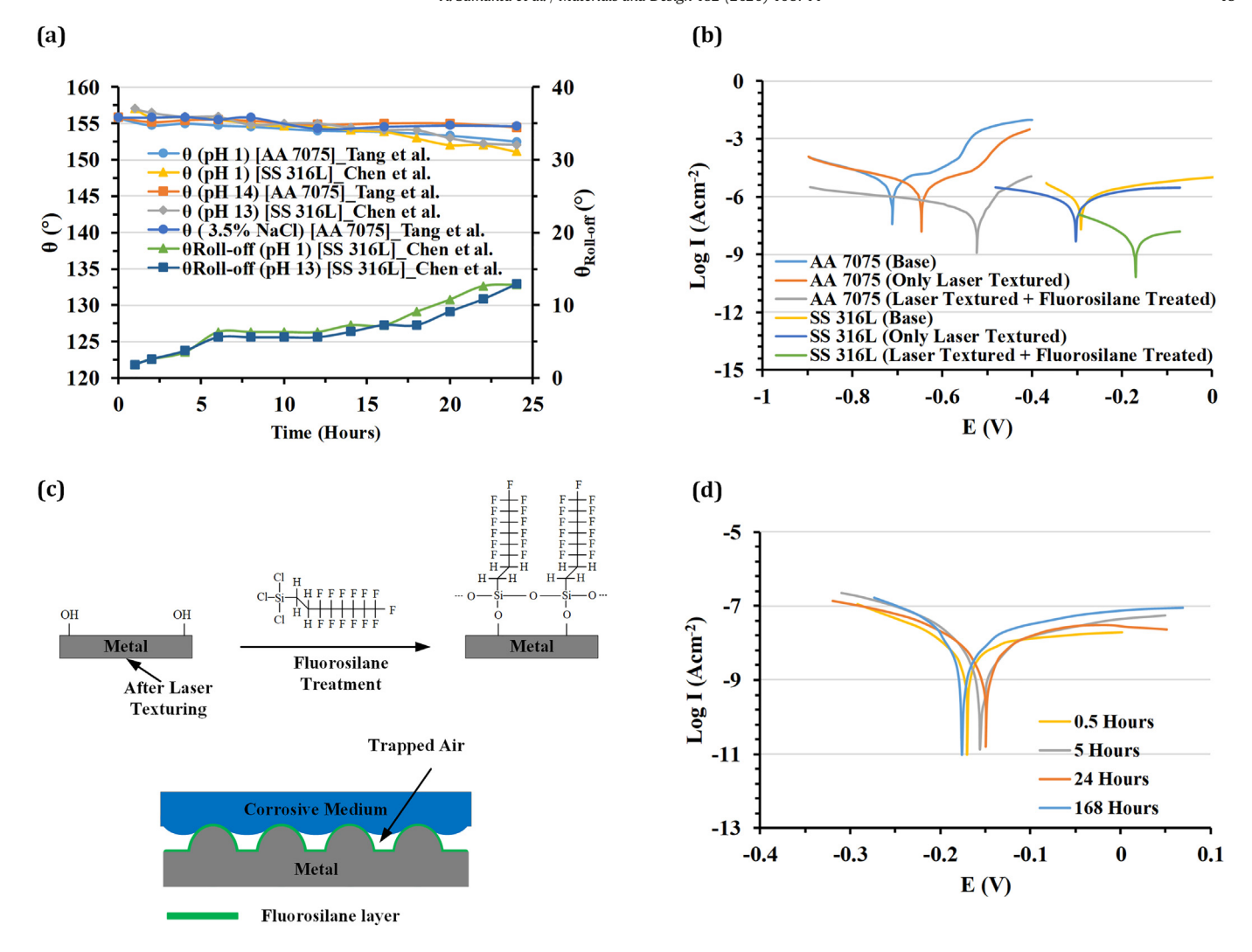


Fig. 14. Stability and durability of laser textured and chemically modified metal surface for corrosion resistance: (a) Variation of θ_w and $\theta_{Roll-off}$ against time for acidic (pH = 1), alkaline (pH = 13–14) and NaCl (3.5%) solution, plotted by the author from data reported in [98,225] with permission from RSC and American Scientific Publishers (ASP); (b) The Tafel polarization curves of the base material, only laser textured and laser textured + fluorosilane treated for SS 316L and AA7075 alloys, plotted by the author from data reported in [98,225] with permission from RSC and ASP; (c) Schematic illustration of the effect of the chemistry modified layer and surface textures to improve corrosion resistance; (d) Tafel polarization curves laser textured and fluorosilane treated SS 316L surfaces after different immersion time in 3.5% NaCl aqueous solution, Reproduced from [98] with permission from RSC.

increased from 1 \pm 0.5 to 14.7 \pm 1.3°. However, even after such a long abrasive wear test, the coating still showed a heterogeneous wetting regime with high water repellency. Only a tiny number of nanoparticles were removed after the abrasion test. One important factor contributed towards improved abrasion resistance is related to higher hardness of stainless steel compared to pure titanium. Garcia-Giron et al. [227] later showed that surface hardening prior to laser texturing can improve the abrasion resistance. They performed low-temperature plasma surface carburizing to improve the hardness of stainless steel from 172 to 305 HV. After that, they performed nanosecond laser texturing followed by coating with fluoropolymer. According to the ISO 11998:2006 abrasion test for 300 cycles, carburized stainless steel can retain its wettability better compared to untreated specimens. A comparison of abrasion resistance for laser textured with fluoropolymer coated metal is shown in Table 7.

Several other abrasion tests were reported where superhydrophobic metal surfaces were rubbed against sandpaper at different abrasion distance and applied pressure. However, the type of sandpaper varies across different research groups, including 260 grit [98], 400 grit [222], and 800 grit [225]. Over an abrasion distance of 3 m, laser textured and fluorosilane treated stainless steel, carbon steel, and AA 7075 retained superhydrophobicity after the abrasion test, as shown in Fig. 15a. SS 316L was able to retain its superhydrophobicity till

12.5 kPa pressure for an abrasion distance of 2.5 m. However, AA7075 quickly degrade when the applied pressure was 5 kPa for 3 m abrasion distance (Fig. 15b). During the abrasion test, surface nanostructures were worn out for SS 316L, as shown in Fig. 15c–e. As the abrasion distance increased from 1 m to 2.5 m, more worn out nanostructures can be observed. On the other hand, AA7075 undergoes severely worn tracks when applied pressure increased from 1.5 kPa to 3.0 kPa, as shown in Fig. 15f–h. One shortcoming of the existing abrasion studies lies in the lack of a single standard method to characterize abrasive wear on laser textured surfaces. It makes it challenging to interpret the effect of materials, laser texturing processes, and chemical modification processes on abrasion resistance.

4. Conclusions and future perspective

Emerging laser-based surface texturing methods demonstrate significant potential for manufacturing nanostructured surfaces, with the additional advantages of maintaining high precision and process flexibility. In this review paper, a thorough review of the fundamentals of wettability and different schemes for achieving different categories of wettability through a combination of laser texturing methods and subsequent surface chemistry modification methods is presented. This paper starts with the fundamental theories analyzing that laser textured

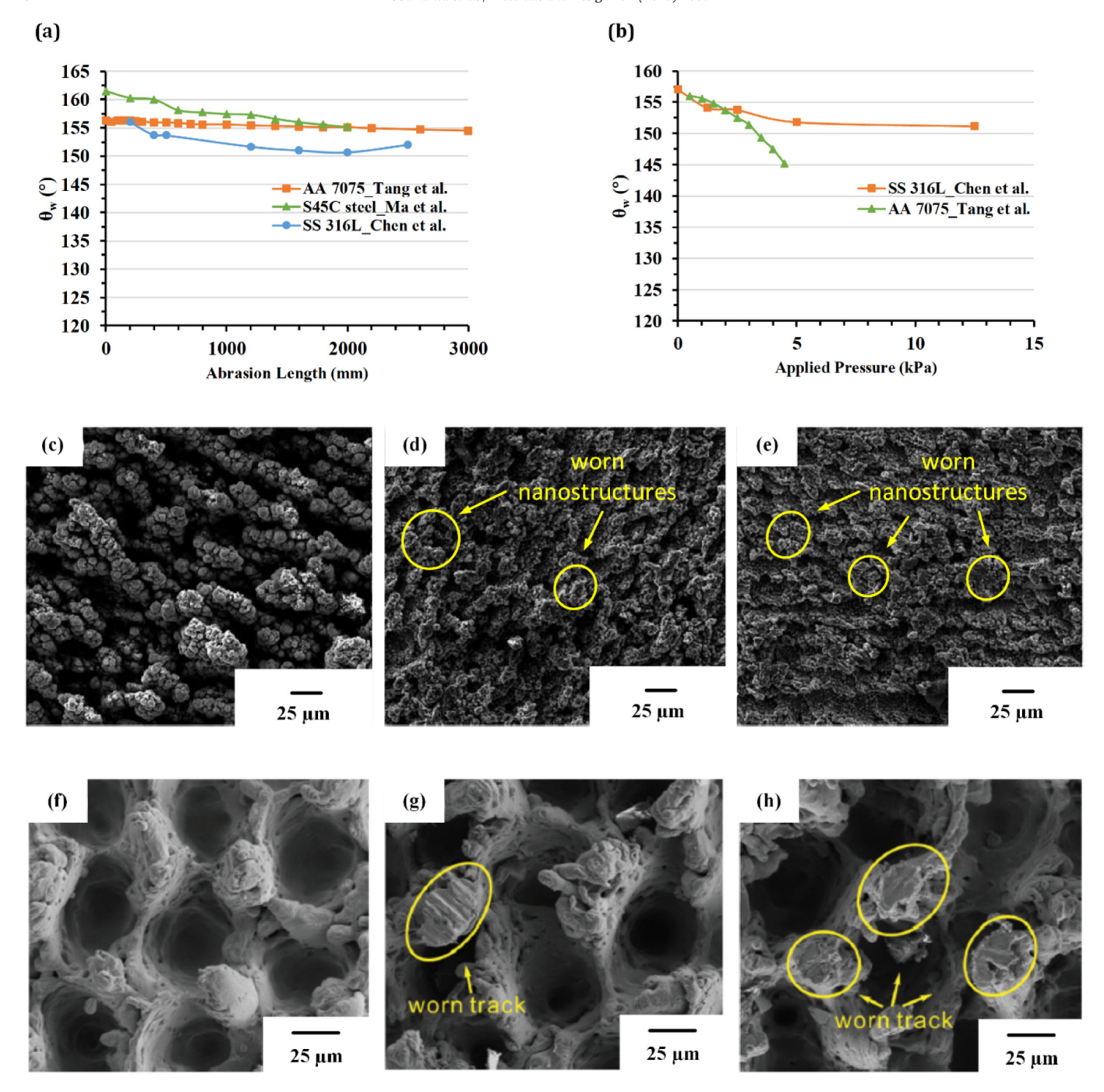


Fig. 15. Durability of laser textured and chemically modified metal surface for of abrasion resistance: (a) Variation of θ_w against abrasion length for SS 316L, AA7075, and S45C steel, plotted by the author from data reported in [98,222,225] with permission from RSC, ASP, and Elsevier; (b) Variation of θ_w against applied pressure for SS 316L and AA7075, plotted by the author from data reported in [98,225] with permission from RSC and ASP; Abraded SS 316L surface (c) before abrasion, (d) after abrasion 1.0 m at the applied pressure of 12.5 kPa and (e) after abrasion 2.5 m at the applied pressure of 12.5 kPa. Reproduced from [98] with permission from RSC; Abraded AA 7075 surface after abrasion for 3.0 m (f) before abrasion, (g) at applied pressure 1.5 kPa and (h) at applied pressure 3.0 kPa. Reproduced from [225] with permission from ASP.

micro/nanostructures alone cannot achieve the desired wettability, and surface chemistry modification plays a critical role as well to decide the final wetting condition. Subsequently, the transition of surface wettability as a complex function of micro/nanostructure generated by laser texturing methods and surface chemistry imposed by the subsequent chemistry modification methods is discussed.

The fabrication of the laser-based processing of micro/nanostructured metal surface with desired wettability is a two-step process: (1) micro-scale, nano-scale or dual-scale surface feature creation by femtosecond/picosecond/nanosecond pulsed lasers and (2) subsequent surface chemistry modification by exposure to air, chemical

treatment, boiling water treatment or heat treatment. This paper concisely summarizes that two types of surface features are created by laser texturing: (a) nanostructures by femtosecond and picosecond laser and (b) hierarchical structures by femtosecond, picosecond, nanosecond and hybrid laser texturing processes. The size and shape of those surface structures are controlled by varying the laser fluence, laser scanning speed and laser spot size. Immediately after laser texturing, the treated surface behaved as superhydrophilic due to a large amount of polar oxide and hydroxide sites accumulated on the treated surface. However, this wetting state is very unstable and changes over time.

Several different surface chemistry modification methods to achieve superhydrophobicity are discussed. Firstly, superhydrophobic wettability can be created on these structured surfaces by storing in air for a long time (10-30 days), which absorbs airborne organic constituents with polar functional end into the active polar sites of the textured surface. Secondly, superhydrophobicity can be achieved on the laser textured surface by chemical treatment with fluoro-silane and long-chain alkyl groups to attach low energy functional groups on top of fabricated micro/nanostructures. Thirdly, superhydrophobicity can be achieved by low-temperature heat treatment to accelerate this absorption process. In addition to superhydrophobicity, surface chemistry is also critical for achieving a superhydrophilic metal surface. Chemical treatment with highly polar nitrile (-CN), carbonyl (-C(=0)-), and carboxyl (-COOH) groups after the laser texturing process helped to achieve superhydrophilic behavior. Stable superhydrophilicity can achieve on the textured aluminum surface by boiling water treatment to create highly polar pseudoboehmite nanostructure on top of micro/nanostructures or high-temperature heat treatment which burns out the absorbed organic constituents.

A combination of laser processing and chemistry modification to achieve various wettabilities still faces several issues that need to be resolved in the future research study. Firstly, existing research on laser texturing mostly focused on surface structure generation and has a deficiency of appreciation of the roles of surface chemistry for laser textured surfaces. Some of the chemistry modification methods lack a thorough investigation of the processing mechanism. The relationship between surface structures and surface chemistry is still under discussion, upon which the researchers can accurately adjust their combination to achieve desired wettability. Secondly, on the theoretical understanding front, the relationship between surface roughness, feature density, size of multiscale structures, and the surface chemical properties in terms of dispersive and non-dispersive components still requires further investigation. In addition, whether the combination of laser texturing and chemical modification can produce surfaces that can sense external agents like glucose level in the blood, biological sensing, etc. Laser texturing has been recently used to modify the surface structure and surface chemistry of polymers for biomedical applications [228]. Therefore, it could be explored for texturing polymer-coated metals. These will open more direction for future research for laser texturing.

Another important issue of laser texturing is associated with the improvement of processing speed and poor process throughput. The lasertexturing community has welcomed exploration of an alternate approach for a long time to improve processing efficiency and reduce production cost [18] while keeping the performance compared with the existing methods. Recent effort [124] has provided a pathway to improve the processing efficiency of single beam laser texturing by defocusing the laser beam and scanning large surface area underwater in each pulse. It is expected that future approaches inspired by this or alternate approaches will be explored, which can significantly improve the processing efficiency and generate both nanoscale and hierarchical structures. Another strategy can be explored by means of a multilaser/multi-beam approach or a single-laser/multi-beam approach or a combination of both [229]. The multi-laser/multi-beam concept is based on a lateral arrangement of multiple lasers and pulse pickers, whereas a single-laser/multi-beam concept is based on a lateral splitting of one laser and one multi-channel pulse picker.

Durability and stability are the other two crucial aspects that need to be investigated thoroughly. Existing studies show that a laser textured surface combined with fluorosilane treatment shows excellent chemical stability, corrosion, and abrasion resistance. Other chemistry modification methods should also be investigated for stability and durability so that the optimum surface chemistry modification method can be practiced for future research. Other durability studies, including particle contamination, bacterial contamination, and biofouling, should be studied. More exploration of these new approaches, durability, and stability

studies will be beneficial for future acceptance of laser texturing for commercial usage to process large surface areas for industrial applications.

CRediT authorship contribution statement

Avik Samanta:Investigation, Visualization, Writing - original draft, Writing - review & editing.**Qinghua Wang:**Investigation.**Scott K. Shaw:**Writing - review & editing.**Hongtao Ding:**Conceptualization, Methodology, Writing - review & editing, Supervision, Funding acquisition.

Declaration of competing interest

The authors declare that they have no known competing financial interests or personal relationships that could have appeared to influence the work reported in this paper.

Acknowledgments

The authors gratefully acknowledge the financial support provided by the National Science Foundation under Grant Number #1762353.

References

- W. Barthlott, C. Neinhuis, Purity of the sacred lotus, or escape from contamination in biological surfaces, Planta 202 (1997) 1–8, https://doi.org/10.1007/ s004250050096.
- [2] L. Feng, Y. Zhang, J. Xi, Y. Zhu, N. Wang, F. Xia, L. Jiang, Petal effect: a superhydrophobic state with high adhesive force, Langmuir 24 (2008) 4114–4119, https://doi.org/10.1021/LA703821H.
- [3] K. Koch, B. Bhushan, W. Barthlott, Diversity of structure, morphology and wetting of plant surfaces, Soft Matter 4 (2008) 1943–1963, https://doi.org/10.1039/ b804854a.
- [4] K. Koch, B. Bhushan, W. Barthlott, Multifunctional surface structures of plants: an inspiration for biomimetics, Prog. Mater. Sci. 54 (2009) 137–178, https://doi.org/ 10.1016/j.pmatsci.2008.07.003.
- [5] X.-Q. Feng, X. Gao, Z. Wu, L. Jiang, Q.-S. Zheng, Superior water repellency of water strider legs with hierarchical structures: experiments and analysis, Langmuir 23 (2007) 4892–4896, https://doi.org/10.1021/la063039b.
- [6] Z.-Z. Gu, H. Uetsuka, K. Takahashi, R. Nakajima, H. Onishi, A. Fujishima, O. Sato, Structural color and the lotus effect, Angew. Chemie - Int. Ed. 42 (2003) 894–897, https://doi.org/10.1117/12.2245933.
- [7] D. Byun, J. Hong, Saputra, J.H. Ko, Y.J. Lee, H.C. Park, B.K. Byun, J.R. Lukes, Wetting characteristics of insect wing surfaces, J. Bionic Eng. 6 (2009) 63–70, https://doi. org/10.1016/S1672-6529(08)60092-X.
- [8] H.M. Chen, C.K. Chen, R.S. Liu, L. Zhang, J. Zhang, D.P. Wilkinson, Nano-architecture and material designs for water splitting photoelectrodes, Chem. Soc. Rev. 41 (2012) 5654–5671, https://doi.org/10.1039/c2cs35019j.
- [9] C. Meng, B. Wang, Z. Gao, Z. Liu, Q. Zhang, J. Zhai, Insight into the role of surface wettability in dlectrocatalytic hydrogen evolution reactions using light-sensitive nanotubular TiO₂ supported Pt electrodes, Sci. Rep. 7 (2017) 1–8, https://doi.org/ 10.1038/srep41825.
- [10] J.B. Habedank, F.J. Günter, N. Billot, R. Gilles, T. Neuwirth, G. Reinhart, M.F. Zaeh, Rapid electrolyte wetting of lithium-ion batteries containing laser structured electrodes: in situ visualization by neutron radiography, Int. J. Adv. Manuf. Technol. (2019)https://doi.org/10.1007/s00170-019-03347-4.
- [11] D.H. Jeon, Wettability in electrodes and its impact on the performance of lithiumion batteries, Energy Storage Mater 18 (2019) 139–147, https://doi.org/10.1016/j. ensm.2019.01.002.
- [12] L. Guo, G.H. Tang, Dropwise condensation on bioinspired hydrophilic-slippery surface, RSC Adv. 8 (2018) 39341–39351, https://doi.org/10.1039/c8ra08190e.
- [13] M. Pang, X. Liu, K. Liu, Effect of wettability on the friction of a laser-textured cemented carbide surface in dilute cutting fluid, Adv. Mech. Eng. 9 (2017) 1–9, https://doi.org/10.1177/1687814017738154.
- [14] D. Jafari, W.W. Wits, B.J. Geurts, Metal 3D-printed wick structures for heat pipe application: Capillary performance analysis, Applied Thermal Engineering 143 (2018) 403–414, https://doi.org/10.1016/j.applthermaleng.2018.07.111.
- [15] J. Hong, S. Kurt, A. Thor, A hydrophilic dental implant surface exhibit thrombogenic properties in vitro, Clin. Implant. Dent. Relat. Res. 15 (2013) 105–112, https://doi. org/10.1111/j.1708-8208.2011.00362.x.
- [16] S. Ferraris, A. Bobbio, M. Miola, S. Spriano, Micro- and nano-textured, hydrophilic and bioactive titanium dental implants, Surf. Coatings Technol. 276 (2015) 374–383, https://doi.org/10.1016/j.surfcoat.2015.06.042.
- [17] M. Ferrari, A. Benedetti, E. Santini, F. Ravera, L. Liggieri, E. Guzman, F. Cirisano, Biofouling control by superhydrophobic surfaces in shallow euphotic seawater, Colloids Surfaces A Physicochem. Eng. Asp. 480 (2015) 369–375, https://doi.org/10.1016/j.colsurfa.2014.11.009.

- [18] K. Bartlet, S. Movafaghi, L.P. Dasi, A.K. Kota, K.C. Popat, Antibacterial activity on superhydrophobic titania nanotube arrays, Colloids Surfaces B Biointerfaces. (2018)https://doi.org/10.1016/j.colsurfb.2018.03.019.
- [19] X. Zhao, M.J. Blunt, J. Yao, Pore-scale modeling: effects of wettability on waterflood oil recovery, J. Pet. Sci. Eng. 71 (2010) 169–178, https://doi.org/10.1016/j.petrol. 2010.01.011.
- [20] J. Yang, Z. Zhang, X. Xu, X. Zhu, X. Men, X. Zhou, Superhydrophilic-superoleophobic coatings, J. Mater. Chem. 22 (2012) 2834, https://doi.org/10.1039/c2jm15987b.
- [21] M.A. Samaha, H.V. Tafreshi, M. Gad-el-Hak, Superhydrophobic surfaces: from the lotus leaf to the submarine, Comptes Rendus - Mec 340 (2012) 18–34, https:// doi.org/10.1016/j.crme.2011.11.002.
- [22] J.W. Gose, K. Golovin, M. Boban, J.M. Mabry, A. Tuteja, M. Perlin, S.L. Ceccio, Characterization of superhydrophobic surfaces for drag reduction in turbulent flow, J. Fluid Mech. 845 (2018) 560–580, https://doi.org/10.1017/jfm.2018.210.
- [23] D. Wei, J. Wang, H. Wang, Y. Liu, S. Li, D. Li, Anti-corrosion behaviour of superwetting structured surfaces on Mg-9Al-1Zn magnesium alloy, Appl. Surf. Sci. 483 (2019) 1017–1026, https://doi.org/10.1016/j.apsusc.2019.03.286.
- [24] B.K. Tudu, A. Kumar, B. Bhushan, Facile approach to develop anti-corrosive superhydrophobic aluminium with high mechanical, chemical and thermal durability, Philos. Trans. R. Soc. A Math. Phys. Eng. Sci. 377 (2019)https://doi.org/10. 1098/rsta.2018.0272.
- [25] H. Wang, Y. Zhu, Z. Hu, X. Zhang, S. Wu, R. Wang, Y. Zhu, A novel electrodeposition route for fabrication of the superhydrophobic surface with unique self-cleaning, mechanical abrasion and corrosion resistance properties, Chem. Eng. J. 303 (2016) 37–47, https://doi.org/10.1016/j.cej.2016.05.133.
- [26] S.S. Latthe, P. Sudhagar, A. Devadoss, A.M. Kumar, S. Liu, C. Terashima, K. Nakata, A. Fujishima, A mechanically bendable superhydrophobic steel surface with self-cleaning and corrosion-resistant properties, J. Mater. Chem. A 3 (2015) 14263–14271, https://doi.org/10.1039/c5ta02604k.
- [27] Y. Liu, L. Li, H. Li, H. Hu, An experimental study of surface wettability effects on dynamic ice accretion process over an UAS propeller model, Aerosp. Sci. Technol. 73 (2018) 164–172, https://doi.org/10.1016/j.ast.2017.12.003.
- [28] L. Cao, A.K. Jones, V.K. Sikka, J. Wu, D. Gao, Anti-icing superhydrophobic coatings, Langmuir 25 (2009) 12444–12448, https://doi.org/10.1021/la902882b.
- [29] I.U. Vakarelski, N.A. Patankar, J.O. Marston, D.Y.C. Chan, S.T. Thoroddsen, Stabilization of Leidenfrost vapour layer by textured superhydrophobic surfaces, Nature 489 (2012) 274–277, https://doi.org/10.1038/nature11418.
- [30] A.R. Betz, J. Jenkins, C.J. Kim, D. Attinger, Boiling heat transfer on superhydrophilic, superhydrophobic, and superbiphilic surfaces, Int. J. Heat Mass Transf. 57 (2013) 733–741, https://doi.org/10.1016/j.ijheatmasstransfer.2012.10.080.
- [31] H. Gau, S. Herminghaus, P. Lenz, R. Lipowsky, Liquid morphologies on structured surfaces: from microchannels to microchips, Science (80-.) 283 (1999) 46–49, https://doi.org/10.1126/science.283.5398.46.
- [32] S.J. Park, M.K. Seo, Solid-liquid Interface, Interface Sci. Compos, Elsevier, Amsterdam, The Netherlands 2011, pp. 147–252, https://doi.org/10.1016/B978-0-12-375049-5.00003-7.
- [33] K. Koch, W. Barthlott, Superhydrophobic and superhydrophilic plant surfaces: an inspiration for biomimetic materials, Philos. Trans. R. Soc. A Math. Phys. Eng. Sci. 367 (2009) 1487–1509, https://doi.org/10.1098/rsta.2009.0022.
- [34] A.Y. Vorobyev, C. Guo, Making human enamel and dentin surfaces superwetting for enhanced adhesion, Appl. Phys. Lett. 99 (2011) 2009–2012, https://doi.org/ 10.1063/1.3660579.
- [35] A.Y. Vorobyev, C. Guo, Metal pumps liquid uphill, Appl. Phys. Lett. 94 (2009) https://doi.org/10.1063/1.3117237.
- [36] A.Y. Vorobyev, C. Guo, Water sprints uphill on glass, J. Appl. Phys. 108 (2010) 10–14, https://doi.org/10.1063/1.3511431.
- [37] A.Y. Vorobyev, C. Guo, Laser turns silicon superwicking, Opt. Express 18 (2010) 6455–6460, https://doi.org/10.1364/0E.18.006455.
- [38] A.Y. Vorobyev, C. Guo, Superwicking surfaces produced by femtosecond laser, Adv. Lasers 2015, pp. 101–115, https://doi.org/10.1007/978-94-017-9481-7.
- [39] Z. Chu, S. Seeger, Superamphiphobic surfaces, Chem. Soc. Rev. 43 (2014) 2784–2798, https://doi.org/10.1039/C3CS60415B.
- [40] L. Gao, T.J. McCarthy, Contact angle hysteresis explained, Langmuir 22 (2006) 6234–6237, https://doi.org/10.1021/la060254j.
- [41] B. Bhushan, Y.C. Jung, Wetting, adhesion and friction of superhydrophobic and hydrophilic leaves and fabricated micro/nanopatterned surfaces, J. Phys. Condens. Matter. 20 (2008), 225010. https://doi.org/10.1088/0953-8984/20/22/225010.
- [42] J. Kijlstra, K. Reihs, A. Klamt, Roughness and topology of ultra-hydrophobic surfaces, Colloids Surfaces A Physicochem. Eng. Asp. 206 (2002) 521–529, https://doi.org/10.1016/S0927-7757(02)00089-4.
- [43] A. He, W. Liu, W. Xue, H. Yang, Y. Cao, Nanosecond laser ablated copper superhydrophobic surface with tunable ultrahigh adhesion and its renewability with low temperature annealing, Appl. Surf. Sci. 434 (2018) 120–125, https:// doi.org/10.1016/j.apsusc.2017.10.143.
- [44] B. Bhushan, E.K. Her, Fabrication of superhydrophobic surfaces with high and low adhesion inspired from rose petal, Langmuir 26 (2010) 8207–8217, https://doi. org/10.1021/la904585j.
- [45] J. Long, P. Fan, D. Gong, D. Jiang, H. Zhang, L. Li, M. Zhong, Superhydrophobic surfaces fabricated by femtosecond laser with tunable water adhesion: from lotus leaf to rose petal, ACS Appl. Mater. Interfaces 7 (2015) 9858–9865, https://doi.org/10.1021/acsami.5b01870.
- [46] B. Bhushan, M. Nosonovsky, The rose petal effect and the modes of superhydrophobicity, Philos. Trans. R. Soc. A. 368 (2010) 4713–4728, https://doi. org/10.1098/rsta.2010.0203.
- [47] R.N. Wenzel, Resistance of solid surfaces to wetting by water, Ind. Eng. Chem. 28 (1936) 988–994, https://doi.org/10.1021/ie50320a024.

- [48] B.A.B.D. Cassie, S. Baxter, Wettability of porous surfaces, Trans. Faraday Soc. 40 (1944) 546–551, https://doi.org/10.1039/TF9444000546.
- [49] A. Marmur, Wetting on hydrophobic rough surfaces: to be heterogeneous or not to be? Langmuir 19 (2003) 8343.
- [50] P. Lv, Y. Xue, Y. Shi, H. Lin, H. Duan, Metastable states and wetting transition of sub-merged superhydrophobic structures, Phys. Rev. Lett. 112 (2014) 1–5, https://doi.org/10.1103/PhysRevLett.112.196101.
- [51] E. Jiaqiang, Y. Jin, Y. Deng, W. Zuo, X. Zhao, D. Han, Q. Peng, Z. Zhang, Wetting models and working mechanisms of typical surfaces existing in nature and their application on superhydrophobic surfaces: a review, Adv. Mater. Interfaces 5 (2018) 1–39, https://doi.org/10.1002/admi.201701052.
- [52] L. Duta, A.C. Popescu, I. Zgura, N. Preda, I.N. Mihailescu, Wettability of nanostructured surfaces, Wetting and Wettability 2015, pp. 207–252, https://doi.org/10.5772/32009
- [53] R.N. Wenzel, Surface roughness and contact angle, J. Phys. Colloid Chem. 53 (1949) 1466–1467, https://doi.org/10.1021/j150474a015.
- [54] J. Bico, C. Tordeux, D. Quere, Rough wetting, Eur. Lett. 55 (2001) 214–220, https://doi.org/10.1209/epl/i2001-00402-x.
- [55] G. McHale, N.J. Shirtcliffe, S. Aqil, C.C. Perry, M.I. Newton, Topography driven spreading, Phys. Rev. Lett. 93 (2004)https://doi.org/10.1103/PhysRevLett.93. 036102 (036102-1)
- [56] K.M. Hay, M.I. Dragila, J. Liburdy, Theoretical model for the wetting of a rough surface, J. Colloid Interface Sci. 325 (2008) 472–477, https://doi.org/10.1016/j.jcis. 2008.06.004.
- [57] Z. Han, Z. Mu, W. Yin, W. Li, S. Niu, J. Zhang, L. Ren, Biomimetic multifunctional surfaces inspired from animals, Adv. Colloid Interf. Sci. 234 (2016) 27–50, https://doi.org/10.1016/j.cis.2016.03.004.
- [58] H. Liu, L. Feng, J. Zhai, L. Jiang, D. Zhu, Reversible wettability of a chemical vapor deposition prepared ZnO film between superhydrophobicity and superhydrophilicity, Langmuir 20 (2004) 5659–5661, https://doi.org/10.1021/1a036280o.
- [59] R. De Sun, A. Nakajima, A. Fujishima, T. Watanabe, K. Hashimoto, Photoinduced surface wettability conversion of ZnO and TiO₂ thin films, J. Phys. Chem. B 105 (2001) 1984–1990, https://doi.org/10.1021/jp002525j.
- [60] J.D. Eick, L.N. Johnson, J.R. Fromer, R.J. Good, A.W. Neumann, Surface topography: its influence on wetting and adhesion in a dental adhesive system, J. Dent. Res. 51 (1972) 780–788, https://doi.org/10.1177/00220345720510031401.
- [61] F.Ç. Cebeci, Z. Wu, L. Zhai, R.E. Cohen, M.F. Rubner, Nanoporosity-driven superhydrophilicity: a means to create multifunctional antifogging coatings, Langmuir 22 (2006) 2856–2862, https://doi.org/10.1021/la053182p.
- [62] P. Roach, N.J. Shirtcliffe, M.I. Newton, Progess in superhydrophobic surface development, Soft Matter 4 (2008) 224, https://doi.org/10.1039/b712575p.
- [63] T. Sun, L. Feng, X. Gao, L. Jiang, Bioinspired surfaces with special wettability, Acc. Chem. Res. 38 (2005) 644–652, https://doi.org/10.1021/ar040224c.
- [64] X. Zhang, F. Shi, J. Niu, Y. Jiang, Z. Wang, Superhydrophobic surfaces: from structural control to functional application, J. Mater. Chem. 18 (2008) 621–633, https://doi.org/10.1039/b711226b.
- [65] E. Celia, T. Darmanin, E. Taffin de Givenchy, S. Amigoni, F. Guittard, Recent advances in designing superhydrophobic surfaces, J. Colloid Interface Sci. 402 (2013) 1–18, https://doi.org/10.1016/j.jcis.2013.03.041.
- [66] S. Wang, L. Feng, L. Jiang, One-step solution-immersion process for the fabrication of stable bionic superhydrophobic surfaces, Adv. Mater. 18 (2006) 767–770, https://doi.org/10.1002/adma.200501794.
- [67] S. Chen, C. Hu, L. Chen, N. Xu, Facile fabrication of superhydrophobic surface from micro/nanostructure metal alkanethiolate based films, Chem. Commun. 200 (2007) 1919–1921, https://doi.org/10.1039/b700994a.
- [68] A.Y. Vorobyev, C. Guo, Multifunctional surfaces produced by femtosecond laser pulses, J. Appl. Phys. 117 (2015)https://doi.org/10.1063/1.4905616.
- [69] M.V. Rukosuyev, J. Lee, S.J. Cho, G. Lim, M.B.G. Jun, One-step fabrication of superhydrophobic hierarchical structures by femtosecond laser ablation, Appl. Surf. Sci. 313 (2014) 411–417, https://doi.org/10.1016/j.apsusc.2014. 05.224.
- [70] J. Song, S. Huang, K. Hu, Y. Lu, X. Liu, W. Xu, Fabrication of superoleophobic surfaces on Al substrates, J. Mater. Chem. A 1 (2013) 14783–14789, https://doi.org/10. 1039/c3ta13807k.
- [71] D.V. Ta, A. Dunn, T.J. Wasley, R.W. Kay, J. Stringer, P.J. Smith, C. Connaughton, J.D. Shephard, Nanosecond laser textured superhydrophobic metallic surfaces and their chemical sensing applications, Appl. Surf. Sci. 357 (2015) 248–254, https://doi.org/10.1016/j.apsusc.2015.09.027.
- [72] R. Jagdheesh, M. Diaz, J.L. Ocaña, Bio inspired self-cleaning ultrahydrophobic aluminium surface by laser processing, RSC Adv. 6 (2016) 72933–72941, https://doi.org/10.1039/C6RA12236A.
- [73] S. Ji, P.A. Ramadhianti, T.B. Nguyen, W.D. Kim, H. Lim, Simple fabrication approach for superhydrophobic and superoleophobic Al surface, Microelectron. Eng. 111 (2013) 404–408, https://doi.org/10.1016/j.mee.2013.04.010.
- [74] J. Ou, W. Hu, S. Liu, M. Xue, F. Wang, W. Li, Superoleophobic textured copper surfaces fabricated by chemical etching/oxidation and surface fluorination, ACS Appl. Mater. Interfaces 5 (2013) 10035–10041, https://doi.org/10.1021/ am402531m.
- [75] J. Ryu, K. Kim, J.Y. Park, B.G. Hwang, Y.C. Ko, H.J. Kim, J.S. Han, E.R. Seo, Y.J. Park, S.J. Lee, Nearly perfect durable superhydrophobic surfaces fabricated by a simple one-step plasma treatment, Sci. Rep. 7 (2017) 1–8, https://doi.org/10.1038/s41598-017-02108-1.
- [76] B. Li, H. Li, L. Huang, N. Ren, X. Kong, Femtosecond pulsed laser textured titanium surfaces with stable superhydrophilicity and superhydrophobicity, Appl. Surf. Sci. 389 (2016) 585–593, https://doi.org/10.1016/j.apsusc.2016.07.137.

- [77] R. Jagdheesh, Fabrication of a Superhydrophobic Al₂O₃ surface using picosecond laser pulses, Langmuir 30 (2014) 12067–12073, https://doi.org/10.1021/ la5033527.
- [78] C.V. Ngo, D.M. Chun, Fast wettability transition from hydrophilic to superhydrophobic laser-textured stainless steel surfaces under low-temperature annealing, Appl. Surf. Sci. 409 (2017) 232–240, https://doi.org/10.1016/j.apsusc. 2017.03.038
- [79] H.J. Choi, S. Choo, J.H. Shin, K.I. Kim, H. Lee, Fabrication of superhydrophobic and oleophobic surfaces with overhang structure by reverse nanoimprint lithography, J. Phys. Chem. C 117 (2013) 24354–24359, https://doi.org/10. 1021/jp4070399.
- [80] P.M. Hansson, A. Swerin, J. Schoelkopf, P.A.C. Gane, E. Thormann, Influence of surface topography on the interactions between nanostructured hydrophobic surfaces, Langmuir 28 (2012) 8026–8034, https://doi.org/10.1021/la300628m.
- [81] E. Bormashenko, T. Stein, G. Whyman, Y. Bormashenko, R. Pogreb, Wetting properties of the multiscaled nanostructured polymer and metallic superhydrophobic surfaces, Langmuir 22 (2006) 9982–9985, https://doi.org/10.1021/la061622m.
- [82] T. Darmanin, F. Guittard, Superoleophobic surfaces with short fluorinated chains? Soft Matter 9 (2013) 5982–5990, https://doi.org/10.1039/c3sm50643f.
- [83] H. Bellanger, T. Darmanin, E. Taffin De Givenchy, F. Guittard, Influence of intrinsic oleophobicity and surface structuration on the superoleophobic properties of PEDOP films bearing two fluorinated tails, J. Mater. Chem. A 1 (2013) 2896–2903, https://doi.org/10.1039/c2ta00517d.
- [84] A. Dramé, T. Darmanin, S.Y. Dieng, E.T. De Givenchy, F. Guittard, Superhydrophobic and oleophobic surfaces containing wrinkles and nanoparticles of PEDOT with two short fluorinated chains, RSC Adv. 4 (2014) 10935–10943, https://doi.org/10.1039/ c3ra47479h.
- [85] T. Darmanin, J. Tarrade, E. Celia, F. Guittard, Superoleophobic meshes with high adhesion by electrodeposition of conducting polymer containing short perfluorobutyl chains, J. Phys. Chem. C 118 (2014) 2052–2057, https://doi.org/10.1021/jp410639j.
- [86] J. Tarrade, T. Darmanin, E.T. De Givenchy, F. Guittard, Super liquid-repellent properties of electrodeposited hydrocarbon and fluorocarbon copolymers, RSC Adv. 3 (2013) 10848–10853, https://doi.org/10.1039/c3ra40636a.
- [87] A.K. Kota, A. Tuteja, Superoleophobic surfaces, ACS Symp. Ser. 1106 (2012) 171–185, https://doi.org/10.1021/bk-2012-1106.ch011.
- [88] R. Menini, M. Farzaneh, Elaboration of Al₂O₃/PTFE icephobic coatings for protecting aluminum surfaces, Surf. Coatings Technol. 203 (2009) 1941–1946, https://doi.org/ 10.1016/j.surfcoat.2009.01.030.
- [89] J. Bravo, L. Zhai, Z. Wu, R.E. Cohen, M.F. Rubner, Transparent superhydrophobic films based on silica nanoparticles, Langmuir 23 (2007) 7293–7298, https://doi. org/10.1021/la070159q.
- [90] L. Zhai, F.C. Cebeci, R.E. Cohen, M.F. Rubner, Stable superhydrophobic coatings from polyelectrolyte multilayers, Nano Lett. 4 (2004) 1349–1353, https://doi.org/10. 1021/nl049463j.
- [91] Y. Li, X. Zhu, X. Zhou, B. Ge, S. Chen, W. Wu, A facile way to fabricate a superamphiphobic surface, Appl. Phys. A Mater. Sci. Process. 115 (2014) 765–770, https://doi.org/10.1007/s00339-014-8438-8.
- [92] M.H. Kwon, H.S. Shin, C.N. Chu, Fabrication of a super-hydrophobic surface on metal using laser ablation and electrodeposition, Appl. Surf. Sci. 288 (2014) 222–228, https://doi.org/10.1016/j.apsusc.2013.10.011.
- [93] Y. Xiu, Y. Liu, D.W. Hess, C.P. Wong, Mechanically robust superhydrophobicity on hierarchically structured Si surfaces, Nanotechnology 21 (2010)https://doi.org/ 10.1088/0957-4484/21/15/155705.
- [94] T. Sun, G. Wang, H. Liu, L. Feng, L. Jiang, D. Zhu, Control over the wettability of an aligned carbon nanotube film, J. Am. Chem. Soc. 125 (2003) 14996–14997, https://doi.org/10.1021/ja038026o.
- [95] G. Hayase, K. Kanamori, G. Hasegawa, A. Maeno, H. Kaji, K. Nakanishi, A superamphiphobic macroporous silicone monolith with marshmallow-like flexibility, Angew. Chemie - Int. Ed. 52 (2013) 10788–10791, https://doi.org/10.1002/ anje 2013/04169
- [96] T. Furuta, M. Sakai, T. Isobe, A. Nakajima, Effect of dew condensation on the wettability of rough hydrophobic surfaces coated with two different silanes, Langmuir 26 (2010) 13305–13309, https://doi.org/10.1021/la101663a.
- [97] M. Rahimi, P. Fojan, L. Gurevich, A. Afshari, Effects of aluminium surface morphology and chemical modification on wettability, Appl. Surf. Sci. 296 (2014) 124–132, https://doi.org/10.1016/j.apsusc.2014.01.059.
- [98] T. Chen, H.H. Liu, H. Yang, W. Yan, W. Zhu, H.H. Liu, Biomimetic fabrication of robust self-assembly superhydrophobic surfaces with corrosion resistance properties on stainless steel substrate, RSC Adv. 6 (2016) 43937–43949, https://doi.org/10. 1039/C6RA06500G.
- [99] B. Liu, G. Jiang, W. Wang, X. Mei, K. Wang, J. Cui, J. Wang, Porous microstructures induced by picosecond laser scanning irradiation on stainless steel surface, Opt. Lasers Eng. 78 (2016) 55–63, https://doi.org/10.1016/j.optlaseng.2015.10.003.
- [100] J. Long, M. Zhong, H. Zhang, P. Fan, Superhydrophilicity to superhydrophobicity transition of picosecond laser microstructured aluminum in ambient air, J. Colloid Interface Sci. 441 (2015) 1–9, https://doi.org/10.1016/j.jcis.2014.11.015.
- [101] J. Long, P. Fan, M. Zhong, H. Zhang, Y. Xie, C. Lin, Superhydrophobic and colorful copper surfaces fabricated by picosecond laser induced periodic nanostructures, Appl. Surf. Sci. 311 (2014) 461–467, https://doi.org/10.1016/j.apsusc.2014.05.090.
- [102] F. Chen, D. Zhang, Q. Yang, J. Yong, G. Du, J. Si, F. Yun, X. Hou, Bioinspired wetting surface via laser microfabrication, ACS Appl. Mater. Interfaces 5 (2013) 6777–6792, https://doi.org/10.1021/am401677z.
- [103] A. Gupta, M.R. Joshi, N. Mahato, K. Balani, Superhydrophobic surfaces, Biosurfaces A Mater. Sci. Eng. Perspect. 11 (2015) 170–200, https://doi.org/10.1002/ 9781118950623.ch6.

- [104] J. Jeevahan, M. Chandrasekaran, G. Britto Joseph, R.B. Durairaj, G. Mageshwaran, Superhydrophobic surfaces: a review on fundamentals, applications, and challenges, J. Coatings Technol. Res. 15 (2018) 231–250, https://doi.org/10.1007/ s11998-017-0011-x
- [105] J.T. Simpson, S.R. Hunter, T. Aytug, Superhydrophobic materials and coatings: a review, Reports Prog. Phys. 78 (2015)https://doi.org/10.1088/0034-4885/78/8/086501
- [106] G. Barati Darband, M. Aliofkhazraei, S. Khorsand, S. Sokhanvar, A. Kaboli, Science and engineering of Superhydrophobic surfaces: review of corrosion resistance, chemical and mechanical stability, Arab. J. Chem. (2018)https://doi.org/10.1016/j. arabic.2018.01.013.
- [107] A. Milionis, E. Loth, I.S. Bayer, Recent advances in the mechanical durability of superhydrophobic materials, Adv. Colloid Interf. Sci. 229 (2016) 57–79, https:// doi.org/10.1016/j.cis.2015.12.007.
- [108] Y.Y. Yan, N. Gao, W. Barthlott, Mimicking natural superhydrophobic surfaces and grasping the wetting process: a review on recent progress in preparing superhydrophobic surfaces, Adv. Colloid Interf. Sci. 169 (2011) 80–105, https:// doi.org/10.1016/j.cis.2011.08.005.
- [109] P. Zhang, F.Y. Lv, A review of the recent advances in superhydrophobic surfaces and the emerging energy-related applications, Energy 82 (2015) 1068–1087, https:// doi.org/10.1016/j.energy.2015.01.061.
- [110] J. Drelich, E. Chibowski, Superhydrophilic and superwetting surfaces: definition and mechanisms of control, Langmuir 26 (2010) 18621–18623, https://doi.org/ 10.1021/la1039893.
- [111] J. Drelich, E. Chibowski, D.D. Meng, K. Terpilowski, Hydrophilic and superhydrophilic surfaces and materials, Soft Matter 7 (2011) 9804–9828, https://doi.org/10.1039/c1sm05849e.
- [112] J. Zhang, S.J. Severtson, Fabrication and use of artificial superhydrophilic surfaces, J. Adhes. Sci. Technol. 28 (2014) 751–768, https://doi.org/10.1080/01694243.2012. 697725.
- [113] L. Zhang, N. Zhao, J. Xu, Fabrication and application of superhydrophilic surfaces: a review, J. Adhes. Sci. Technol. 28 (2014) 769–790, https://doi.org/10.1080/ 01694243.2012.697714.
- [114] X. Feng, L. Jiang, Design and creation of superwetting/antiwetting surfaces, Adv. Mater. 18 (2006) 3063–3078, https://doi.org/10.1002/adma.200501961.
- [115] T.A. Otitoju, A.L. Ahmad, B.S. Ooi, Superhydrophilic (superwetting) surfaces: a review on fabrication and application, J. Ind. Eng. Chem. 47 (2017) 19–40, https://doi.org/10.1016/j.jiec.2016.12.016.
- [116] E. Stratakis, Nanomaterials by ultrafast laser processing of surfaces, Sci. Adv. Mater. 4 (2012) 407–431.
- [117] A.M. Kietzig, S.G. Hatzikiriakos, P. Englezos, Patterned superhydrophobic metallic surfaces, Langmuir 25 (2009) 4821–4827, https://doi.org/10.1021/la8037582.
- [118] P. Bizi-Bandoki, S. Valette, E. Audouard, S. Benayoun, Time dependency of the hydrophilicity and hydrophobicity of metallic alloys subjected to femtosecond laser irradiations, Appl. Surf. Sci. 273 (2013) 399–407, https://doi.org/10.1016/j.apsusc. 2013.02.054.
- [119] Y. Tian, L. Jiang, Wetting: intrinsically robust hydrophobicity, Nat. Mater. 12 (2013) 291–292, https://doi.org/10.1038/nmat3610.
- [120] H. Yan, M.R.B.A. Rashid, S.Y. Khew, F. Li, M. Hong, Wettability transition of laser textured brass surfaces inside different mediums, Appl. Surf. Sci. 427 (2018) 369–375, https://doi.org/10.1016/j.apsusc.2017.08.218.
- [121] F. Chen, D. Zhang, Q. Yang, X. Wang, B. Dai, X. Li, X. Hao, Y. Ding, J. Si, X. Hou, Anisotropic wetting on microstrips surface fabricated by femtosecond laser, Langmuir 27 (2011) 359–365, https://doi.org/10.1021/la103293j.
- [122] M.Y. Shen, C.H. Crouch, J.E. Carey, E. Mazur, Femtosecond laser-induced formation of submicrometer spikes on silicon in water, Appl. Phys. Lett. 85 (2004) 5694–5696, https://doi.org/10.1063/1.1828575.
- [123] O. Varlamova, F. Costache, M. Ratzke, J. Reif, Control parameters in pattern formation upon femtosecond laser ablation, Appl. Surf. Sci. 253 (2007) 7932–7936, https://doi.org/10.1016/j.apsusc.2007.02.067.
- [124] Q. Wang, A. Samanta, S.K. Shaw, H. Hu, H. Ding, Nanosecond laser-based high-throughput surface nanostructuring (nHSN), Appl. Surf. Sci. 507 (2020) 145136, https://doi.org/10.1016/j.apsusc.2004.11.001.
- [125] D.H. Kam, S. Bhattacharya, J. Mazumder, Control of the wetting properties of an AISI 316L stainless steel surface by femtosecond laser-induced surface modification, J. Micromechanics Microengineering. 22 (2012), 105019. https://doi.org/10. 1088/0960-1317/22/10/105019.
- [126] P. Pou, J. del Val, A. Riveiro, R. Comesaña, F. Arias-González, F. Lusquiños, M. Bountinguiza, F. Quintero, J. Pou, Laser texturing of stainless steel under different processing atmospheres: from superhydrophilic to superhydrophobic surfaces, Appl. Surf. Sci. 475 (2019) 896–905, https://doi.org/10.1016/j.apsusc.2018.12.248.
- [127] A.Y. Vorobyev, C. Guo, Femtosecond laser structuring of titanium implants, Appl. Surf. Sci. 253 (2007) 7272–7280, https://doi.org/10.1016/j.apsusc.2007.03.006.
- [128] A.Y. Vorobyev, V.S. Makin, C. Guo, Periodic ordering of random surface nanostructures induced by femtosecond laser pulses on metals, J. Appl. Phys. 101 (2007) https://doi.org/10.1063/1.2432288.
- [129] R. Jagdheesh, J.J. García-Ballesteros, J.L. Ocaña, One-step fabrication of near superhydrophobic aluminum surface by nanosecond laser ablation, Appl. Surf. Sci. 374 (2016) 2–11, https://doi.org/10.1016/j.apsusc.2015.06.104.
- [130] A.Y. Vorobyev, C. Guo, Femtosecond laser nanostructuring of metals, Opt. InfoBase Conf. Pap. 14 (2006) 2164–2169.
- [131] D. Huerta-Murillo, A.I. Aguilar-Morales, S. Alamri, J.T. Cardoso, R. Jagdheesh, A.F. Lasagni, J.L. Ocaña, Fabrication of multi-scale periodic surface structures on Ti-6Al-4V by direct laser writing and direct laser interference patterning for modified wettability applications, Opt. Lasers Eng. 98 (2017) 134–142, https://doi.org/10.1016/j.optlaseng.2017.06.017.

- [132] D. Huerta-Murillo, A. García-Girón, J.M. Romano, J.T. Cardoso, F. Cordovilla, M. Walker, S.S. Dimov, J.L. Ocaña, Wettability modification of laser-fabricated hierarchical surface structures in Ti-6Al-4V titanium alloy, Appl. Surf. Sci. 463 (2019) 838–846, https://doi.org/10.1016/j.apsusc.2018.09.012.
- [133] A. Samanta, Q. Wang, S.K. Shaw, H. Ding, Nanostructuring of laser textured surface to achieve superhydrophobicity on engineering metal surface, J. Laser Appl. 31 (2019), 022515. https://doi.org/10.2351/1.5096148.
- [134] H.M. Van Driel, J.E. Sipe, J.F. Young, Laser-induced periodic surface structure on solids: a universal phenomenon, Phys. Rev. Lett. 49 (1982) 1955–1958, https:// doi.org/10.1103/PhysRevLett.49.1955.
- [135] J. Bonse, S. Hohm, S.V. Kirner, A. Rosenfeld, J. Kruger, Laser-induced periodic surface structures-a scientific Evergreen, IEEE J. Sel. Top. Quantum Electron. 23 (2017)https://doi.org/10.1109/JSTQE.2016.2614183.
- [136] M. Birnbaum, Semiconductor surface damage produced by ruby lasers, J. Appl. Phys. 36 (1965) 3688–3689, https://doi.org/10.1063/1.1703071.
- [137] J. Bonse, J. Krüger, S. Höhm, A. Rosenfeld, Femtosecond laser-induced periodic surface structures, Journal Laser Appl 24 (2012) 042006, https://doi.org/10.2351/1. 4712658
- [138] R. Jagdheesh, B. Pathiraj, E. Karatay, G.R.B.E. Römer, A.J. Huis In'T Veld, Laser-induced nanoscale superhydrophobic structures on metal surfaces, Langmuir 27 (2011) 8464–8469, https://doi.org/10.1021/la2011088.
- [139] J. Bonse, S. Baudach, J. Krüger, W. Kautek, M. Lenzner, Femtosecond laser ablation of silicon-modification thresholds and morphology, Appl. Phys. A Mater. Sci. Process. 74 (2002) 19–25, https://doi.org/10.1007/s003390100893.
- [140] J.E. Sipe, J.F. Young, J.S. Preston, H.M. Van Driel, Laser-induced periodic surface structure. I. Theory, Phys. Rev. B 27 (1983) 1141–1154, https://doi.org/10.1103/ PhysRevB.27.1141.
- [141] F. Garrelie, O. Parriaux, N. Faure, S. Tonchev, S. Reynaud, F. Pigeon, M. Bounhalli, J.-P. Colombier, Evidence of surface plasmon resonance in ultrafast laser-induced ripples, Opt. Express 19 (2011) 9035, https://doi.org/10.1364/oe.19.009035.
- [142] M. Huang, F. Zhao, Y. Cheng, N. Xu, Z. Xu, Origin of laser-induced nearsubwavelength ripples: interference between surface plasmons and incident laser, ACS Nano 3 (2009) 4062–4070, https://doi.org/10.1021/nn900654v.
- [143] G. Miyaji, K. Miyazaki, Origin of periodicity in nanostructuring on thin film surfaces ablated with femtosecond laser pulses, Opt. Express 16 (2008), 16265. https://doi. org/10.1364/oe.16.016265.
- [144] K.M. Tanvir Ahmmed, C. Grambow, A.M. Kietzig, Fabrication of micro/nano structures on metals by femtosecond laser micromachining, Micromachines 5 (2014) 1219–1253, https://doi.org/10.3390/mi5041219.
- [145] B. Wu, M. Zhou, J. Li, X. Ye, G. Li, L. Cai, Superhydrophobic surfaces fabricated by microstructuring of stainless steel using a femtosecond laser, Appl. Surf. Sci. 256 (2009) 61–66, https://doi.org/10.1016/j.apsusc.2009.07.061.
- [146] A. Cunha, A.P. Serro, V. Oliveira, A. Almeida, R. Vilar, M.C. Durrieu, Wetting behaviour of femtosecond laser textured Ti-6Al-4V surfaces, Appl. Surf. Sci. 265 (2013) 688–696, https://doi.org/10.1016/j.apsusc.2012.11.085.
- [147] P. Bizi-Bandoki, S. Benayoun, S. Valette, B. Beaugiraud, E. Audouard, Modifications of roughness and wettability properties of metals induced by femtosecond laser treatment, Appl. Surf. Sci. 257 (2011) 5213–5218, https://doi.org/10.1016/j. apsusc.2010.12.089.
- [148] M. Groenendijk, J. Meijer, Microstructuring using femtosecond pulsed laser ablation, J. Laser Appl. 18 (2006) 227–235, https://doi.org/10.2351/1.2227020.
- [149] A.Y. Vorobyev, C. Guo, Colorizing metals with femtosecond laser pulses, Appl. Phys. Lett. 92 (2008) 1–4, https://doi.org/10.1063/1.2834902.
- [150] S. Sakabe, M. Hashida, S. Tokita, S. Namba, K. Okamuro, Mechanism for self-formation of periodic grating structures on a metal surface by a femtosecond laser pulse, Phys. Rev. B Condens. Matter Mater. Phys. 79 (2009) 1–4, https://doi.org/10.1103/PhysRevB.79.033409.
- [151] M. Tsukamoto, K. Asuka, H. Nakano, M. Hashida, M. Katto, N. Abe, M. Fujita, Periodic microstructures produced by femtosecond laser irradiation on titanium plate, Vacuum 80 (2006) 1346–1350, https://doi.org/10.1016/j.vacuum.2006.01. 016.
- [152] K. Okamuro, M. Hashida, Y. Miyasaka, Y. Ikuta, S. Tokita, S. Sakabe, Laser fluence dependence of periodic grating structures formed on metal surfaces under femtosecond laser pulse irradiation, Phys. Rev. B Condens. Matter Mater. Phys. 82 (2010) 1–5, https://doi.org/10.1103/PhysRevB.82.165417.
- [153] C.A. Zuhlke, T.P. Anderson, D.R. Alexander, Fundamentals of layered nanoparticle covered pyramidal structures formed on nickel during femtosecond laser surface interactions, Appl. Surf. Sci. 283 (2013) 648–653, https://doi.org/10.1016/j. apsusc.2013.07.002.
- [154] Z. Zhang, Q. Gu, W. Jiang, H. Zhu, K. Xu, Y. Ren, C. Xu, Achieving of bionic superhydrophobicity by electrodepositing nano-Ni-pyramids on the picosecond laserablated micro-cu-cone surface, Surf. Coatings Technol. 363 (2019) 170–178, https://doi.org/10.1016/j.surfcoat.2019.02.037.
- [155] J. Long, L. Pan, P. Fan, D. Gong, D. Jiang, H. Zhang, L. Li, M. Zhong, Cassie-state stability of metallic superhydrophobic surfaces with various micro/nanostructures produced by a femtosecond laser, Langmuir 32 (2016) 1065–1072, https://doi. org/10.1021/acs.langmuir.5b04329.
- [156] M. Martínez-Calderon, A. Rodríguez, A. Dias-Ponte, M.C. Morant-Miñana, M. Gómez-Aranzadi, S.M. Olaizola, Femtosecond laser fabrication of highly hydrophobic stainless steel surface with hierarchical structures fabricated by combining ordered microstructures and LIPSS, Appl. Surf. Sci. 374 (2016) 81–89, https://doi.org/10.1016/j.apsusc.2015.09.261.
- [157] V.D. Ta, A. Dunn, T.J. Wasley, J. Li, R.W. Kay, J. Stringer, P.J. Smith, E. Esenturk, C. Connaughton, J.D. Shephard, Laser textured surface gradients, Appl. Surf. Sci. 371 (2016) 583–589, https://doi.org/10.1016/j.apsusc.2016.03.054.

- [158] D.M. Chun, C.V. Ngo, K.M. Lee, Fast fabrication of superhydrophobic metallic surface using nanosecond laser texturing and low-temperature annealing, CIRP Ann. Manuf. Technol. 65 (2016) 519–522, https://doi.org/10.1016/j.cirp.2016.04.019.
- [159] A.Y. Vorobyev, C. Guo, Direct femtosecond laser surface nano/microstructuring and its applications, Laser Photonics Rev. 7 (2013) 385–407, https://doi.org/10.1002/ lpor.201200017.
- [160] Q. Wang, A. Samanta, F. Toor, S. Shaw, H. Ding, Colorizing Ti-6Al-4V surface via high-throughput laser surface nanostructuring, J. Manuf. Process. (2019) 70–75, https://doi.org/10.1016/i.imapro.2019.03.050 Elsevier.
- [161] Y. Liu, Z. Zhang, H. Hu, H. Hu, A. Samanta, Q. Wang, H. Ding, An experimental study to characterize a surface treated with a novel laser surface texturing technique: water repellency and reduced ice adhesion, Surf. Coatings Technol. 374 (2019) 634–644, https://doi.org/10.1016/j.surfcoat.2019.06.046.
- [162] L. Gao, T.J. McCarthy, The "lotus effect" explained: two reasons why two length scales of topography are important, Langmuir 22 (2006) 2966–2967, https://doi.org/10.1021/Ja0532149
- [163] L. Feng, S. Li, Y. Li, H. Li, L. Zhang, J. Zhai, Y. Song, B. Liu, L. Jiang, D. Zhu, Super-hydrophobic surfaces: from natural to artificial, Adv. Mater. 14 (2002) 1857–1860, https://doi.org/10.1002/adma.200290020.
- [164] S. Wang, L. Jiang, Definition of superhydrophobic states, Adv. Mater. 19 (2007) 3423–3424, https://doi.org/10.1002/adma.200700934.
- [165] J.-D. Brassard, D.K. Sarkar, J. Perron, Fluorine based superhydrophobic coatings, Appl. Sci. 2 (2012) 453–464, https://doi.org/10.3390/app2020453.
- [166] B. Subramanian, N. Kim, W. Lee, D.A. Spivak, D.E. Nikitopoulos, R.L. McCarley, S.A. Soper, Surface modification of droplet polymeric microfluidic devices for the stable and continuous generation of aqueous droplets, Langmuir 27 (2011) 7949–7957, https://doi.org/10.1002/bmb.20244.DNA.
- [167] A. Achour, M. Islam, S. Solaymani, S. Vizireanu, K. Saeed, G. Dinescu, Influence of plasma functionalization treatment and gold nanoparticles on surface chemistry and wettability of reactive-sputtered TiO₂ thin films, Appl. Surf. Sci. 458 (2018) 678–685, https://doi.org/10.1016/j.apsusc.2018.07.145.
- [168] A.P. Kharitonov, L.N. Kharitonova, Surface modification of polymers by direct fluorination: a convenient approach to improve commercial properties of polymeric articles, Pure Appl. Chem. 81 (2009) 451–471, https://doi.org/10.1351/PAC-CON-08-06-02.
- [169] F.M. Chang, S.L. Cheng, S.J. Hong, Y.J. Sheng, H.K. Tsao, Superhydrophilicity to superhydrophobicity transition of CuO nanowire films, Appl. Phys. Lett. 96 (2010) 2008–2011, https://doi.org/10.1063/1.3360847.
- [170] L.B. Boinovich, A.M. Emelyanenko, K.A. Emelyanenko, A.G. Domantovsky, A.A. Shiryaev, Comment on "Nanosecond laser textured superhydrophobic metallic surfaces and their chemical sensing applications" by Duong V. Ta, Andrew Dunn, Thomas J. Wasley, Robert W. Kay, Jonathan Stringer, Patrick J. Smith, Colm Connaughton, Jonathan D. Shephard, Ap, Appl. Surf. Sci. 379 (2016) 111–113, https://doi.org/10.1016/j.apsusc.2016.04.056.
- [171] C.V. Ngo, D.M. Chun, Effect of heat treatment temperature on the wettability transition from hydrophilic to superhydrophobic on laser-ablated metallic surfaces, Adv. Eng. Mater. 20 (2018) 1–11, https://doi.org/10.1002/adem.201701086.
- [172] C.V. Ngo, D.M. Chun, Control of laser-ablated aluminum surface wettability to superhydrophobic or superhydrophilic through simple heat treatment or water boiling post-processing, Appl. Surf. Sci. 435 (2018) 974–982, https://doi.org/10. 1016/j.apsusc.2017.11.185.
- [173] J.E. O'Gara, B.A. Alden, C.A. Gendreau, P.C. Iraneta, T.H. Walter, Dependence of cyano bonded phase hydrolytic stability on ligand structure and solution pH, J. Chromatogr. A 893 (2000) 245–251, https://doi.org/10.1016/S0021-9673(00) 00696-8.
- [174] P. Horcajada, A. Rámila, G. Férey, M. Vallet-Regí, Influence of superficial organic modification of MCM-41 matrices on drug delivery rate, Solid State Sci. 8 (2006) 1243–1249, https://doi.org/10.1016/j.solidstatesciences.2006.04.016.
- [175] N. Liu, Y. Yao, J.J. Cha, M.T. McDowell, Y. Han, Y. Cui, Functionalization of silicon nanowire surfaces with metal-organic frameworks, Nano Res. 5 (2012) 109–116, https://doi.org/10.1007/s12274-011-0190-1.
- [176] A. Samanta, Q. Wang, G. Singh, S.K. Shaw, F. Toor, A. Ratner, H. Ding, Nanosecond pulsed laser processing turns engineering metal alloys antireflective and superwicking, J. Manuf. Process. 54 (2020) 28–37, https://doi.org/10.1016/j. jmapro.2020.02.029.
- [177] P. Gregorčič, B. Šetina-Batič, M. Hočevar, Controlling the stainless steel surface wettability by nanosecond direct laser texturing at high fluences, Appl. Phys. A Mater. Sci. Process. 123 (2017) 1–8, https://doi.org/10.1007/s00339-017-1392-5.
- [178] V.D. Ta, A. Dunn, T.J. Wasley, J. Li, R.W. Kay, J. Stringer, P.J. Smith, E. Esenturk, C. Connaughton, J.D. Shephard, Laser textured superhydrophobic surfaces and their applications for homogeneous spot deposition, Appl. Surf. Sci. 365 (2016) 153–159, https://doi.org/10.1016/j.apsusc.2016.01.019.
- [179] J.T. Cardoso, A. Garcia-Girón, J.M. Romano, D. Huerta-Murillo, R. Jagdheesh, M. Walker, S.S. Dimov, J.L. Ocaña, Influence of ambient conditions on the evolution of wettability properties of an IR-, ns-laser textured aluminium alloy, RSC Adv. 7 (2017) 39617–39627, https://doi.org/10.1039/c7ra07421b.
- [180] Z. Yang, Y.L. Tian, C.J. Yang, F.J. Wang, X.P. Liu, Modification of wetting property of Inconel 718 surface by nanosecond laser texturing, Appl. Surf. Sci. 414 (2017) 313–324, https://doi.org/10.1016/j.apsusc.2017.04.050.
- [181] M.M. Gentleman, J.A. Ruud, Role of hydroxyls in oxide wettability, Langmuir 26 (2010) 1408–1411, https://doi.org/10.1021/la903029c.
- [182] G. Azimi, R. Dhiman, H.M. Kwon, A.T. Paxson, K.K. Varanasi, Hydrophobicity of rare-earth oxide ceramics, Nat. Mater. 12 (2013) 315–320, https://doi.org/10. 1038/nmar3545.
- [183] J. Hahn, Organic constituents of natural aerosols, Ann. N. Y. Acad. Sci. 338 (1980) 359–376, https://doi.org/10.1111/j.1749-6632.1980.tb19367.x.

- [184] G. Ketseridis, J. Hahn, R. Jaenicke, C. Junge, The organic constituents of atmospheric particulate matter, Atmos. Environ. 10 (1976) 603–610, https://doi.org/10.1016/ 0004-6981(76)90045-7.
- [185] A.H. Goldstein, I.E. Galbally, Known and unexplored organic constituents in the earth's atmosphere, Environ. Sci. Technol. 41 (2007) 1514–1521, https://doi.org/ 10.1021/es072476p.
- [186] S. Shibuichi, T. Yamamoto, T. Onda, K. Tsujii, Super water- and oil-repellent surfaces resulting from fractal structure, J. Colloid Interface Sci. 208 (1998) 287–294, https://doi.org/10.1006/jcis.1998.5813.
- [187] A. Pendurthi, S. Movafaghi, W. Wang, S. Shadman, A.P. Yalin, A.K. Kota, Fabrication of nanostructured omniphobic and superomniphobic surfaces with inexpensive CO₂ laser engraver, ACS Appl. Mater. Interfaces 9 (2017) 25656–25661, https:// doi.org/10.1021/acsami.7b06924.
- [188] A. Steele, B.K. Nayak, A. Davis, M.C. Gupta, E. Loth, S. Adam, K.N. Barada, D. Alexander, C.G. Mool, L. Eric, Linear abrasion of a titanium superhydrophobic surface prepared by ultrafast laser microtexturing, J. Micromechanics Microengineering. 23 (2013) 115012, https://doi.org/10.1088/0960-1317/23/11/15012
- [189] S. Moradi, S. Kamal, P. Englezos, S.G. Hatzikiriakos, Femtosecond laser irradiation of metallic surfaces: effects of laser parameters on superhydrophobicity, Nanotechnology 24 (2013), 415302. https://doi.org/10.1088/0957-4484/24/41/415302.
- [190] J. Lai, B. Sunderland, J. Xue, S. Yan, W. Zhao, M. Folkard, B.D. Michael, Y. Wang, Study on hydrophilicity of polymer surfaces improved by plasma treatment, Appl. Surf. Sci. 252 (2006) 3375–3379, https://doi.org/10.1016/j.apsusc.2005.05. 038
- [191] K.N. Pandiyaraj, V. Selvarajan, R.R. Deshmukh, C. Gao, Modification of surface properties of polypropylene (PP) film using DC glow discharge air plasma, Appl. Surf. Sci. 255 (2009) 3965–3971, https://doi.org/10.1016/j.apsusc.2008.10.090.
- [192] N.Y. Cui, N.M.D. Brown, Modification of the surface properties of a polypropylene (PP) film using an air dielectric barrier discharge plasma, Appl. Surf. Sci. 189 (2002) 31–38, https://doi.org/10.1016/S0169-4332(01)01035-2.
- [193] Z.K. Wang, H.Y. Zheng, C.P. Lim, Y.C. Lam, Polymer hydrophilicity and hydrophobicity induced by femtosecond laser direct irradiation, Appl. Phys. Lett. 95 (2009) https://doi.org/10.1063/1.3232212.
- [194] M.K. Tang, X.J. Huang, Z. Guo, J.G. Yu, X.W. Li, Q.X. Zhang, Fabrication of robust and stable superhydrophobic surface by a convenient, low-cost and efficient laser marking approach, Colloids Surfaces A Physicochem. Eng. Asp. 484 (2015) 449–456, https://doi.org/10.1016/j.colsurfa.2015.08.029.
- [195] H. Ding, Q. Wang, A. Samanta, N. Shen, Nanosecond Laser-based High-throughput Surface Nano-structuring (nHSN) Process, US20190054571A1, 2019.
- [196] F.H. Rajab, C.M. Liauw, P.S. Benson, L. Li, K.A. Whitehead, Picosecond laser treatment production of hierarchical structured stainless steel to reduce bacterial fouling, Food Bioprod. Process. 109 (2018) 29–40, https://doi.org/10.1016/j.fbp.2018. 02.000
- [197] F.H. Rajab, C.M. Liauw, P.S. Benson, L. Li, K.A. Whitehead, Production of hybrid macro/micro/nano surface structures on Ti₆Al₄V surfaces by picosecond laser surface texturing and their antifouling characteristics, Colloids Surfaces B Biointerfaces 160 (2017) 688–696, https://doi.org/10.1016/j.colsurfb.2017.10.008.
- [198] B. Zheng, G. Jiang, W. Wang, X. Mei, Fabrication of superhydrophilic or superhydrophobic self-cleaning metal surfaces using picosecond laser pulses and chemical fluorination, Radiat. Eff. Defects Solids. 171 (2016) 461–473, https:// doi.org/10.1080/10420150.2016.1211658.
- [199] B.J. Li, L.J. Huang, N.F. Ren, X. Kong, Laser ablation processing of zinc sheets in hydrogen peroxide solution for preparing hydrophobic microstructured surfaces, Mater. Lett. 164 (2016) 384–387, https://doi.org/10.1016/j.matlet.2015.11.035.
- [200] J.C. Love, D.B. Wolfe, M.L. Chabinyc, K.E. Paul, G.M. Whitesides, Self-assembled monolayers of alkanethiolates on palladium are good etch resists, J. Am. Chem. Soc. 124 (2002) 1576–1577, https://doi.org/10.1021/ja012569l.
- [201] J. Christopher Love, D.B. Wolfe, R. Haasch, M.L. Chabinyc, K.E. Paul, G.M. Whitesides, R.G. Nuzzo, Formation and structure of self-assembled monolayers of alkanethiolates on palladium, J. Am. Chem. Soc. 125 (2003) 2597–2609, https://doi.org/10.1021/ja028692+.
- [202] E. Ostuni, L. Yan, G.M. Whitesides, The interaction of proteins and cells with self-assembled monolayers of alkanethiolates on gold and silver, Colloids Surfaces B Biointerfaces 15 (1999) 3–30, https://doi.org/10.1016/S0927-7765(99)00004-1.
- [203] J. Aizenberg, A.J. Black, G.M. Whitesides, Oriented growth of calcite controlled by self-assembled monolayers of functionalized alkanethiols supported on gold and silver, J. Am. Chem. Soc. 121 (1999) 4500–4509, https://doi.org/10.1021/ ja984254k.
- [204] G.B. Sigal, M. Mrksich, G.M. Whitesides, Using surface plasmon resonance spectroscopy to measure the association of detergents with self-assembled monolayers of hexadecanethiolate on gold, Langmuir 13 (2002) 2749–2755, https://doi.org/10.1021/la961024f.
- [205] C.D. Bain, E.B. Troughton, Y.T. Tao, J. Evall, G.M. Whitesides, R.G. Nuzzo, Formation of monolayer films by the spontaneous assembly of organic thiols from solution onto gold, J. Am. Chem. Soc. 111 (1989) 321–335, https://doi.org/10.1021/ ia00183a049.
- [206] P.E. Laibinis, G.M. Whitesides, D.L. Aliara, Y.T. Tao, A.N. Parikh, R.G. Nuzzo, Comparison of the structures and wetting properties of self-assembled monolayers of nalkanethiols on the coinage metal surfaces, cu, ag, au, J. Am. Chem. Soc. 113 (1991) 7152–7167, https://doi.org/10.1021/ja00019a011.

- [207] R.G. Nuzzo, E.M. Korenic, L.H. Dubois, Studies of the temperature-dependent phase behavior of long chain n-alkyl thiol monolayers on gold, J. Chem. Phys. 93 (1990) 767–773, https://doi.org/10.1063/1.459528.
- [208] S. Sarbada, Y.C. Shin, Superhydrophobic contoured surfaces created on metal and polymer using a femtosecond laser, Appl. Surf. Sci. 405 (2017) 465–475, https:// doi.org/10.1016/j.apsusc.2017.02.019.
- [209] X.C. Wang, B. Wang, H. Xie, H.Y. Zheng, Y.C. Lam, Picosecond laser micro/nano surface texturing of nickel for superhydrophobicity, J. Phys. D. Appl. Phys. 51 (2018) 115305. https://doi.org/10.1088/1361-6463/aaad24.
- [210] U. Trdan, M. Hočevar, P. Gregorčič, Transition from superhydrophilic to superhydrophobic state of laser textured stainless steel surface and its effect on corrosion resistance, Corros. Sci. 123 (2017) 21–26, https://doi.org/10.1016/j. corsci.2017.04.005.
- [211] J. Long, Z. Cao, C. Lin, C. Zhou, Z. He, X. Xie, Formation mechanism of hierarchical micro- and nanostructures on copper induced by low-cost nanosecond lasers, Appl. Surf. Sci. 464 (2019) 412–421, https://doi.org/10.1016/j.apsusc.2018.09.055.
- [212] Z. Lian, J. Xu, Z. Yu, P. Yu, H. Yu, A simple two-step approach for the fabrication of bio-inspired superhydrophobic and anisotropic wetting surfaces having corrosion resistance, J. Alloys Compd. 793 (2019) 326–335, https://doi.org/10.1016/j. iallcom.2019.04.169.
- [213] Y. Wan, C. Xi, H. Yu, Fabrication of self-cleaning superhydrophobic surface on stainless steel by nanosecond laser, Mater. Res. Express. 5 (2018), 115002. https://doi. org/10.1088/2053-1591/aadbf2.
- [214] D. Patil, S. Aravindan, M. Kaushal Wasson, V. P. P.V. Rao, Fast fabrication of superhydrophobic titanium alloy as antibacterial surface using nanosecond laser texturing, J. Micro Nano-Manufacturing. 6 (2018) 11002, https://doi.org/10. 1115/1.4038093.
- [215] T.-H. Dinh, C.-V. Ngo, D.-M. Chun, Controlling the wetting properties of superhydrophobic titanium surface fabricated by UV nanosecond-pulsed laser and heat treatment, Nanomaterials 8 (2018) 766, https://doi.org/10.3390/ nano8100766.
- [216] J. Pike, S.W. Chan, F. Zhang, X. Wang, J. Hanson, Formation of stable Cu₂O from reduction of CuO nanoparticles, Appl. Catal. A Gen. 303 (2006) 273–277, https://doi.org/10.1016/j.apcata.2006.02.008.
- [217] G. Wang, T.Y. Zhang, Easy route to the wettability cycling of copper surface between superhydrophobicity and superhydrophilicity, ACS Appl. Mater. Interfaces 4 (2012) 273–279, https://doi.org/10.1021/am2013129.
- [218] A. Strålin, T. Hjertberg, Influence of surface composition on initial hydration of aluminium in boiling water, Appl. Surf. Sci. 74 (1994) 263–275, https://doi.org/10. 1016/0169-4332(94)90007-8.
- [219] L. Li, M. Hong, M. Schmidt, M. Zhong, A. Malshe, B. Huis In Tveld, V. Kovalenko, Laser nano-manufacturing - state of the art and challenges, CIRP Ann. - Manuf. Technol. 60 (2011) 735–755, https://doi.org/10.1016/j.cirp.2011.05.005.
- [220] V. Mortazavi, M.M. Khonsari, On the degradation of superhydrophobic surfaces: a review, Wear. 372–373 (2017) 145–157, https://doi.org/10.1016/j.wear.2016.11.
- [221] E. Vazirinasab, R. Jafari, G. Momen, Application of superhydrophobic coatings as a corrosion barrier: a review, Surf. Coatings Technol. 341 (2018) 40–56, https:// doi.org/10.1016/j.surfcoat.2017.11.053.
- [222] Q. Ma, Z. Tong, W. Wang, G. Dong, Fabricating robust and repairable superhydrophobic surface on carbon steel by nanosecond laser texturing for corrosion protection, Appl. Surf. Sci. 455 (2018) 748–757, https://doi.org/10.1016/j. apsusc.2018.06.033.
- [223] M. Rafieazad, J.A. Jaffer, C. Cui, X. Duan, A. Nasiri, Nanosecond laser fabrication of hydrophobic stainless steel surfaces: the impact on microstructure and corrosion resistance, Materials (Basel) 11 (2018)https://doi.org/10.3390/ma11091577.
- [224] L. Ruiz de Lara, R. Jagdheesh, J.L. Ocana, Corrosion resistance of laser patterned ultrahydrophobic aluminium surface, Mater. Lett. 184 (2016) 100–103, https:// doi.org/10.1016/j.matlet.2016.08.022.
- [225] M.K. Tang, X.J. Huang, J.G. Yu, X.W. Li, Q.X. Zhang, Simple fabrication of large-area corrosion resistant superhydrophobic surface with high mechanical strength property on TiAl-based composite, J. Mater. Process. Technol. 239 (2017) 178–186, https://doi.org/10.1016/j.jmatprotec.2016.08.024.
- [226] A.M. Emelyanenko, F.M. Shagieva, A.G. Domantovsky, L.B. Boinovich, Nanosecond laser micro- and nanotexturing for the design of a superhydrophobic coating robust against long-term contact with water, cavitation, and abrasion, Appl. Surf. Sci. 332 (2015) 513–517, https://doi.org/10.1016/j.apsusc.2015.01.202.
- [227] A. Garcia-Giron, J.M. Romano, A. Batal, B. Dashtbozorg, H. Dong, E.M. Solanas, D.U. Angos, M. Walker, P. Penchev, S.S. Dimov, Durability and wear resistance of laser-textured hardened stainless steel surfaces with hydrophobic properties, Langmuir 35 (2019) 5353–5363, https://doi.org/10.1021/acs.langmuir.9b00398.
- [228] A. Riveiro, A.L.B. Maçon, J. del Val, R. Comesaña, J. Pou, Laser surface texturing of polymers for biomedical applications, Front. Phys. 5 (2018)https://doi.org/10. 3389/fphy.2018.00016.
- [229] S. Bruening, K. Du, M. Jarczynski, G. Jenke, A. Gillner, Ultra-fast laser micro processing by multiple laser spots, Procedia CIRP 74 (2018) 573–580, https://doi.org/10.1016/j.procir.2018.08.084.
- [230] A. Samanta, W. Huang, H. Chaudhry, Q. Wang, S.K. Shaw, H. Ding, Design of Chemical Surface Treatment for Laser Textured Metal Alloy to Achieve Extreme Wetting Behavior, ACS Applied Materials and Interfaces 12 (15) (2020) 18032–18045, https://doi.org/10.1021/acsami.9b21438.